UNIVERSITÀ DEGLI STUDI DI GENOVA

DICCA

Department of Civil, Chemical and Environmental Engineering

THESIS IN ENVIRONMENTAL ENGINEERING:

"Application and testing of statistical methodology for landslide susceptibility assessment in a GIS environment: a case study of the municipality of Genoa"

Supervisor

Prof. Rossella Bovolenta

Prof. Bianca Federici

Prof. Paola Salmona

Candidate

Cristina Rapallini

Academic year 2025/2026

TABLE OF CONTENTS

1. INTRODUCTION

Against a backdrop of increasing human pressure and the intensification of extreme weather events, understanding and modelling the various landslide phenomena are fundamental tools for land-use planning, risk management and the mitigation of potential damage. In particular, to contribute to the development of operational tools to support land-use management, it is very important to identify the areas most at risk of landslides.

The availability of national databases, regulations and technical guidelines contributes to the continuous updating of knowledge, methodological consistency across different institutional levels and the improvement of the effectiveness of landslide risk prevention and mitigation measures. However, as these are highly diverse and constantly evolving phenomena, it is important to integrate existing tools with others that are scalable in terms of space and time and can be rapidly applied, so as to always have an up-to-date view of the situation.

A preliminary and essential component of hydrogeological risk analysis and management is the assessment of susceptibility to landslides, that is, the propensity of an area to trigger gravitational phenomena based on its intrinsic characteristics. Unlike the concept of risk, it is limited to expressing the relative probability that an area may be affected by a mass movement, without considering the time scale or the socio-economic consequences. Accurately assessing a territory's susceptibility to landslides lays the foundations for subsequent reliable analyses and modelling.

In recent decades, advances in spatial analysis techniques and the growing availability of georeferenced data and landslide archives have facilitated the development of quantitative approaches to susceptibility assessment. In particular, the integration of numerical modelling techniques and Geographical Information Systems (GIS) provides various tools for mapping the susceptibility of an area with increasing levels of detail and reliability, although uncertainties remain regarding data quality, the scale of analysis and the transferability of models. The aim of this thesis is to critically apply to the municipality of Genoa a statistical methodology for assessing landslide susceptibility, developed in a GIS environment by the Geomatics Laboratory of the Department of Civil, Chemical and Environmental Engineering at the University of Genoa, as part of the RETURN Extended Partnership (RETURN Foundation, 2026). This methodology uses logistic regression to correlate the characteristics of the territory with past landslides, identifying areas with similar characteristics and potentially a higher probability of developing similar phenomena. At the same time, it highlights the factors that have the greatest influence on the development of such phenomena.

The application to the municipality of Genoa – a human-modified Mediterranean environment

historically characterised by intense rainfall – provides an excellent test bed for assessing the scope, reliability and limitations of this methodology.

The work was divided into two main phases: a preliminary phase, aimed at testing and verifying the functionality of the SALSA.1 scripts using various predisposing factors in order to identify any errors; and a subsequent optimization phase, during which the scripts, after being appropriately refined, were run repeatedly to assess the robustness and reliability of the results.

2. LANDSLIDES

A landslide is defined as a mass movement of rock, earth or debris down a slope (Cruden, 1991: UNESCO WP/WLI). In a landslide, three distinct zones can be identified: the detachment zone, where the material is mobilised and forced to descend to lower elevations; a flow zone; and an accumulation zone, where the mobilised material accumulates.

The initiation of such phenomena results from a combination of physical and mechanical processes acting on the slope, progressively leading it from a state of stable or metastable equilibrium to failure (Varnes, 1978; Terzaghi et al., 1996). In geotechnical terms, the stability of a slope is commonly described by the ratio of the material's shear strength to the shear stresses mobilised along a potential slip surface, expressed through the Mohr–Coulomb failure criterion in terms of effective stresses (Terzaghi et al., 1996; Duncan et al., 2014). When this ratio is less than 1, a condition of instability occurs, leading to the initiation of landslide phenomena.

Overall, the triggering of a landslide can be interpreted as the outcome of a long phase of slope predisposition, linked to the geological, geomorphological and structural characteristics of the slope and characterised by processes of alteration, degradation and structural reorganisation of the materials, followed by the action of one or more short-lived triggering factors that cause the conditions of limit equilibrium to be exceeded (Crozier, 1986; Guzzetti et al., 2007).

Among the main physical processes responsible for triggering landslides, the increase in pore pressure plays a predominant role. Soil saturation resulting from intense or prolonged rainfall (ISPRA, 2018), snowmelt or a rise in the water table leads to a significant reduction in effective stresses and, consequently, in the mobilisable shear strength along potential slip surfaces (Iverson, 2000; Fredlund and Rahardjo, 1993). In partially saturated soils, water infiltration also leads to a progressive loss of matrix suction, resulting in a decrease in apparent cohesion, which in particular favours the triggering of surface landslides and debris flows (Fredlund C Rahardjo, 1993; Guzzetti et al., 2007).

Among the mechanical processes that play a significant role in determining the triggering mechanisms and the type of landslide, we can identify an increase in applied loads and changes in slope geometry, whether due to natural causes or human activity (Cruden and Varnes, 1996; Terzaghi et al., 1996), dynamic stresses of seismic origin and certain erosive phenomena.

2.1 Classification of landslides

The classification of landslides according to Varnes (Varnes, 1978) is based on two main criteria: the type of movement and the type of material.

Depending on the type of kinematics, various types of landslides can be distinguished (Regione Liguria; n.d.).

Falls: the detachment of material from steeply inclined surfaces, such as escarpments and cliffs. The material involved is predominantly rock, but may also include soil or debris. Detachment generally occurs along pre-existing mechanical discontinuities within the rock mass, such as fractures of tectonic or weathering origin, as well as stratification surfaces. On steep slopes, the movement of the unstable mass may initially manifest as a free fall, before continuing through bouncing and rolling. These processes are extremely rapid and sudden; this characteristic makes them particularly dangerous even when involving small quantities of material, as energy is released instantaneously, with potentially highly destructive effects (Regione Liguria, n.d.).

Figure 1. Landslide on the Aurelia road between Vesima and Arenzano (Genoa area) in 202c (source: https://www.today.it/citta/liguria-frana-aurelia-arenzano.html)

Topples: a type of landslide that occurs when a mass of material, usually rock, which is partially detached from the slope, rotates forwards about a point or line at the base of the mass, situated below its centre of gravity. The movement is triggered by a destabilising force, often attributable to the combination of gravity and pressures exerted by fluids present in discontinuities (e.g. pore pressure or freeze-thaw cycles), as well as to processes of weathering and mechanical degradation at the base of the unstable elements. This type of phenomenon is facilitated by the presence of systems of subvertical discontinuities, such as fractures or joints, arranged in such a way as to isolate rock blocks

or columns that are poorly oriented relative to the slope. Tipping may affect individual blocks or groups of adjacent elements and is generally characterised by rapid dynamics, with potentially significant effects on slope hazard.

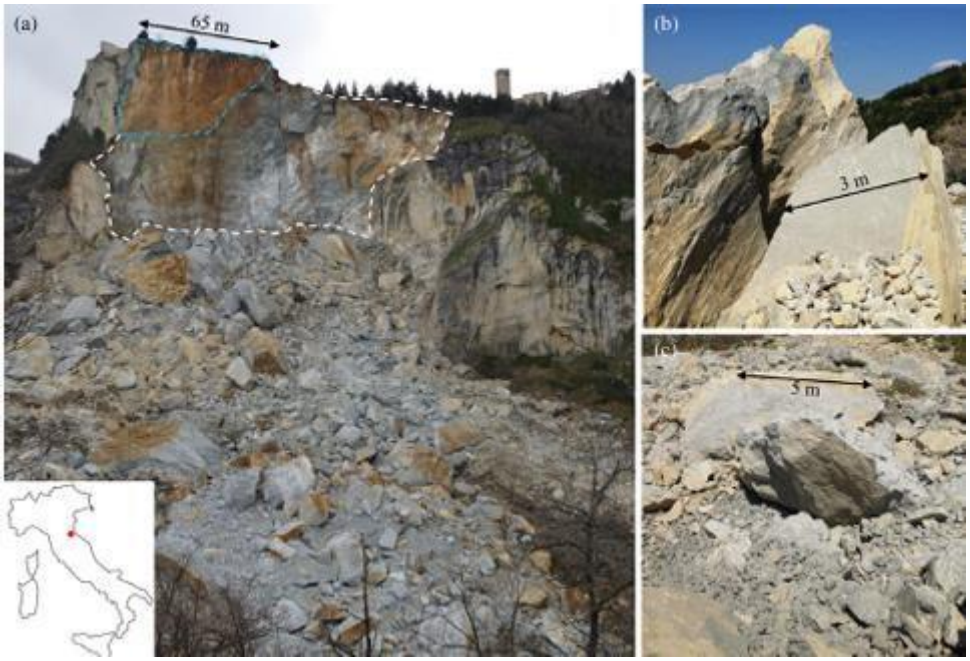

Figure 2. San Leo landslide (Emilia-Romagna) in 2014 (source: Spreafico, Margherita & Franci, Francesca & Bitelli, Gabriele & Borgatti, Lisa & Ghirotti, Monica. (2017). Intact rock bridge breakage and rock mass fragmentation upon failure: Quantification using remote sensing techniques. The Photogrammetric Record. 32. 10.1111/phor.12225.)

Rotational and translational slides: a landslide movement characterised by the displacement of a generally cohesive mass, with little or no internal deformation, along a slide surface or a well-defined shear zone. The material involved consists mainly of soil or debris, whilst the involvement of rock masses is less common and is generally associated with predisposing structural conditions. Depending on the geometry of the slip surface, slides are classified as rotational or translational. In rotational slides, the slip surface has an upward-concave geometry, and the movement of the mass occurs by rotation about a centre located above the landslide body. In this case, in the upper portion of the landslide, the movement is predominantly vertical, whilst in the lower part it progressively evolves into a translational movement towards the valley. Such phenomena are typical of materials exhibiting plastic behaviour, such as clays and silts, and tend to reach a new state of equilibrium, especially when the material redistributes itself along the slope. Translational slides, on the other hand, develop along nearly flat slip surfaces, often controlled by structural discontinuities, stratification surfaces or lithological contacts. The orientation of the slip surface relative to the slope emphasises the tangential component of the acting forces, facilitating the movement of the mass. Conditions particularly conducive to this type of instability include slope-supporting stratifications and the sub-parallel contact with the slope between the bedrock and the overlying materials.

Unlike rotational landslides, which tend to stabilise more readily, translational landslides can remain in a state of persistent instability over time, with the potential for the phenomenon to spread spatially and for subsequent reactivations, particularly in the event of changes in hydrogeological conditions.

Figure 3. Landslide in Via Digione, Genoa in 1988 (source: https://genova.repubblica.it/cronaca/2014/02/0S/foto/via_digione_frana_in_sicurezza_ma_fa_paura_il_ricordo_del_c8-780S2S17/12/?utm_source=chatgpt.com#7)

Rapid and slow flows: landslides characterised by a generally narrow and elongated geometry, which tend to develop along watersheds. The triggering is often linked to the saturation of the material due to the infiltration of rainwater, particularly in clayey or marly strata, resulting in the formation of lobed deposits at the foot of the slope. The movement is associated with widespread internal deformation of the mass and can occur at speeds ranging from very slow to extremely rapid, depending on the geometric and hydrogeological conditions of the slope. Different types are distinguished based on the material involved and the kinematics of the movement. Rock flows involve intensely fractured rock masses that are diffusely deformed. Debris flows are very rapid phenomena involving saturated coarse material, often triggered by intense rainfall or rapid snowmelt. Mudflows involve clayey materials, occur at lower speeds and can develop even on moderate slopes. Mudflows result from the mobilisation of fine-grained materials with a high water content and can reach high speeds. Creep is an extremely slow, continuous or seasonal slope movement affecting the surface portion of the slope, induced by insufficient shear stress not sufficient to cause a fracture, but capable of producing permanent deformations, identifiable through specific morphological indicators (Hungr et al., 2014).

Figure 4. Debris flow in Bardonecchia (TO) 2023 (source: ISPRA, 2024)

Lateral spreads: these are slope movements characterised by a predominantly horizontal component, typically occurring on gently sloping slopes or on almost flat terrain. These phenomena occur when a surface mass moves over a layer of plastic or deformable soil, often consisting of saturated sands or silts susceptible to liquefaction, or of highly deformable cohesive soils. The triggering of this type of landslide may be due to dynamic stresses, such as the passage of seismic waves, or to additional surface loads, which increase the stress on the underlying plastic soil. The movement of the mass is mainly horizontal, and the deformation is accommodated by shear at the base of the expanding mass, as well as the formation of tension fractures in the upper part. Lateral expansions can affect large areas and, although vertical movement is limited, they have significant destructive potential for infrastructure, pipelines and surface structures. Understanding these phenomena requires a combined analysis of soil mechanics, slope geometry and the dynamics of the applied loads, which are fundamental elements for assessing the hazard and associated risk.

Figure 5. Lateral expansion at Nurallao, Sardinia, in 2005 (source: https://www.geopop.it/frane-in-italia-ecco-come-avvengono-e-quali-sono-le-principali-tipologie/)

Complex landslides: these represent phenomena of slope instability in which a combination of two or more movement mechanisms is observed within the same landslide mass. In such cases, a landslide may begin, for example, as a rotational slide, and then evolve into a flow or debris flow, generating hybrid behaviour that is highly variable in space and time. This complexity stems from the heterogeneity of the materials involved, the presence of structural discontinuities, variations in water saturation, and the slope topography, all of which influence the kinematics of the movements. Complex landslides can therefore combine rigid and deformable components, slow and rapid movements, or adjacent stable and unstable areas. From a hazard perspective, complex landslides often represent the most critical phenomena, as their evolution is difficult to predict and can lead to significant impacts on infrastructure and the landscape. Their analysis requires the integration of geomorphological, geotechnical and hydrogeological approaches, supported by monitoring and numerical modelling to estimate possible trajectories, velocities and volumes involved.

Figure c. View from the sea of the Gave landslide: the dotted line indicates the recently reactivated (red) and quiescent (orange) slopes; the old landslide deposit is shown by the black hatched lines. (source: Faccini, 2014)

Each of these classes is then further subdivided, based on the type of material involved in the landslide phenomenon: rock, debris or soil (Table 1).

TIPO DI MOVIMENTO		TIPO DI MATERIALE		
		ROCCIA	SUOLO	
			Grossolano	Fine
CROLLI (falls)		crolli di roccia	crolli di detrito	crolli di terra
RIBALTAMENTI (topples)		ribaltamento di roccia	ribaltamento di detrito	ribaltamento di terra
SCIVOLAMENTI (SLIDES)	ROTAZIONALI	scorrimento di roccia	scorrimento di detrito	scorrimento di terra
	TRASLAZIONALI			
ESPANDIMENTI LATERALI (spreads)		espandimento di roccia	espandimento di detrito	espandimento di terra
COLATE (flows)		flusso di roccia (creep profondo)	colata di detrito (creep superficiale)	colata di terra
FRANE COMPLESSE (complex)		combinazione di due o più tipo di movimento nello spazio e/o nel tempo		

Table 1: Types of landslides: Schematic version of Varnes' classification (1S78) (https://www.iris.unict.it/retrieve/b1f8d814-b082-4cd5-8afe-0c305c58a3e7/3_Cap_2.pdf)

Cruden and Varnes also introduce a classification based on movement velocity, which ranges from extremely slow to extremely fast, a parameter of particular importance in hazard assessment. In practical terms, the correct identification of the type of landslide, the material involved and the velocity regime is an essential step in risk assessment and in defining appropriate mitigation strategies, such as drainage works, stabilisation works and sustainable land management measures.

2.2 Landslide risk

Risk is defined as the possibility that a natural or man-made phenomenon will cause harm to people, settlements, economic activities and infrastructure in a specific area over a given period of time (Department of Civil, n.d.)

Therefore, the risk associated with a catastrophic event can be expressed by the following general formula

$$R = Px\,V\,x\,E$$

Where:

- P = Hazard: the probability that a phenomenon of a given intensity will occur in a over a certain period of time, in a given area. Hazard does not include any information on the potential consequences in terms of damage but represents solely the likelihood of the natural phenomenon occurring.
- V = Vulnerability: the vulnerability of an element (people, buildings, infrastructure, economic activities) is the propensity to suffer damage as a result of the stresses induced by an event of a certain intensity.
- E = Exposure or Exposed Value: this is the number of units (or 'value') of each of the elements at at risk in a given area, such as human lives or settlements.

In the specific field of landslide hazard, hazard is defined as the probability that a landslide event – potentially destructive and characterised by a specific intensity – will occur in a given geographical area within a specified time frame (Varnes, 1984). This definition involves considering the temporal frequency of the event, its intensity and its spatial location, constituting one of the fundamental elements for the geological assessment of areas subject to slope instability.

Time-related aspects, however, are very difficult to incorporate into landslide hazard assessments (Wang, 2024; ISPRA, 2024). At a preliminary stage, it is therefore advisable to consider susceptibility to landslides, i.e. the probability that a landslide event will occur in a specific location, taking into account the combination of geological and environmental factors in a given area (van Westen et al., 2006; Fell et al., 2008).

Susceptibility analysis concerns exclusively the spatial component of the probability of the

phenomenon occurring and does not consider either the temporal frequency of events or their possible consequences.

2.3 Susceptibility assessment

The assessment of landslide susceptibility represents the first step in the broader process of geomorphological risk analysis. In particular, the identification and mapping of areas where slope instability processes have occurred in the past, or which exhibit similar geological and geotechnical characteristics, provide fundamental information for predicting the location of new landslides. Such analyses make it possible to identify potentially unstable areas, providing essential knowledge for spatial planning and risk mitigation (Faccini, 2023).
Susceptibility analysis requires certain basic assumptions (Guzzetti et al., 1999):

i) every landslide event leaves characteristic traces on the ground that can be recognised and mapped through field surveys or remote sensing;
ii) The triggering mechanisms of any landslide phenomenon obey the laws of physics; therefore, identifying the factors contributing to instability enables the development of susceptibility models;
iii) future landslides will occur under the same conditions that caused past landslides;
iv) it is possible to determine the spatial and temporal probability of landslides through the analysis of geological and environmental factors.

Based on these assumptions, a given area can be classified according to different levels of probability of being affected by a specific type of landslide, enabling the production of susceptibility maps that serve as useful decision-support tools for land management and risk prevention.
Various approaches have been developed for assessing landslide susceptibility, which can be broadly categorised into three groups: heuristic methods, deterministic methods and statistical methods (Guzzetti et al., 1999; van Westen et al., 2003; Brenning, 2005; van Westen et al., 2008; Cascini, 2008; Constantin et al., 2011; Neuhäuser et al., 2012; Reid et al., 2015; Chen et al., 2018).

2.3.1 Heuristic methods

Heuristic methods are based on the qualitative or semi-quantitative combination of factors considered significant in determining the spatial distribution and frequency of landslides within a given area. Such approaches require a thorough understanding of the relationships between landslide activity and the geomorphological, geological and environmental characteristics of the

study area.

This knowledge generally derives from field surveys and/or photointerpretation (Canuti et al., 1979; Cardinali et al., 2002), the results of which are subsequently interpreted according to criteria dictated by experience, through procedures that cannot always be formalised. On this basis, an expert identifies the factors predisposing, influencing and determining landslides; they are then divided into classes, to which a weight is assigned representing the greater or lesser propensity to trigger landslide phenomena. The susceptibility map is then obtained by superimposing the thematic maps relating to the various factors considered; each territorial unit is characterised by a susceptibility index equal to the sum of the weights associated with the classes of the individual factors. In some cases, it is also possible to assign a weight to the factors themselves, in order to represent their relative influence: in such cases, the weight of each class is multiplied by the weight of the factor to which it belongs.

The main limitation of this class of methods lies in their subjectivity and their heavy reliance on the availability and quality of field data. However, they allow for the consideration of local characteristics and heterogeneities that are difficult to represent using rigorous mathematical models.

2.3.2 Deterministic methods

Deterministic, or physically based, methods are founded on the application of physical models designed to describe and interpret the mechanisms triggering and driving landslides. Traditionally used for susceptibility zoning in areas of limited extent, these approaches are now also applied to larger geographical contexts. They are based on modelling the physical laws that govern slope stability and involve the calculation of the safety factor for each map unit, enabling its spatial distribution to be represented. The safety factor is defined as the ratio of resisting forces to acting forces along a potential slip surface: values greater than one indicate stable conditions, whilst values less than one indicate unstable situations.

The main parameters considered in the deterministic approach include normal stress, the angle of internal friction of the material, cohesion, neutral pressure, soil thickness, seismic acceleration and external loads. Depending on the type of instability analysed, it is also possible to integrate rainfall infiltration models and complex hydrogeological models, giving rise to so-called physically based models (Montgomery C Dietrich, 1994; Godt et al., 2008). This approach has become widely used thanks to the development of numerous software packages dedicated to susceptibility assessment, including SHALSTAB (Montgomery C Dietrich, 1994), TRIGRS (Baum et al., 2002) and Scoops3D (Reid et al., 2015).

2.3.3 Statistical methods

Statistical methods compare multiple independent variables – that is, the characteristics of the terrain (input parameters) – with the corresponding dependent variable, represented by the presence or absence of landslides. Statistical algorithms seek the optimal relationships and coefficients linking the independent variables to the dependent variable, making these methods particularly suitable for analysing large areas. Statistical methods allow for a quantitative and objective assessment of the contribution of each parameter to the occurrence of a known landslide event. The weights associated with the various factors are in fact calculated using mathematical relationships. Two main subcategories can be distinguished: bivariate methods and multivariate methods. Bivariate methods (Constantin et al., 2011; Chen et al., 2018) analyse individually the relationship between each geological-environmental factor and the landslide catalogue, quantifying the degree of correlation by cross-referencing thematic maps with the landslide map.

Subsequently, various techniques are applied to determine the weight of each factor, including the Weight of Evidence method and the Frequency Ratio (Spiegelhalter, 1986; Bonham-Carter et al., 1989; Neuhäuser et al., 2012). Multivariate methods, on the other hand, allow for the simultaneous assessment of the mutual influence of the various parameters, enabling the estimation of the relative contribution of each variable within an integrated susceptibility model. The most commonly used multivariate techniques include multiple linear regression, discriminant analysis and logistic regression (Guzzetti et al., 2006; Akgun C Türk, 2011). For each of the categories described, there are numerous application methodologies, many of which have been developed relatively recently in conjunction with the spread of Geographic Information Systems (GIS), which have significantly expanded the possibilities for spatial analysis and the management of spatial data (Umar et al., 2014; Chen et al., 2017; Buecchi et al., 2019; Di Napoli et al., 2020).

2.3.4 Determination of map units

In order to produce a landslide susceptibility map, it is first necessary to divide the area under consideration into map units, i.e. spatial sections characterised by a high degree of homogeneity in the geological and environmental parameters deemed relevant for the purposes of the analysis. Each map unit is therefore described by a specific combination of predisposing and conditioning factors, which distinguishes it from adjacent units. The definition of map units represents a crucial stage in the modelling process, as it significantly influences the quality, spatial resolution and reliability of the results obtained. Various criteria for dividing the territory into map units have been proposed in the literature (Guzzetti et al., 1999), each of which is more or less appropriate depending on the scale of analysis, the method adopted and the type of instability considered.

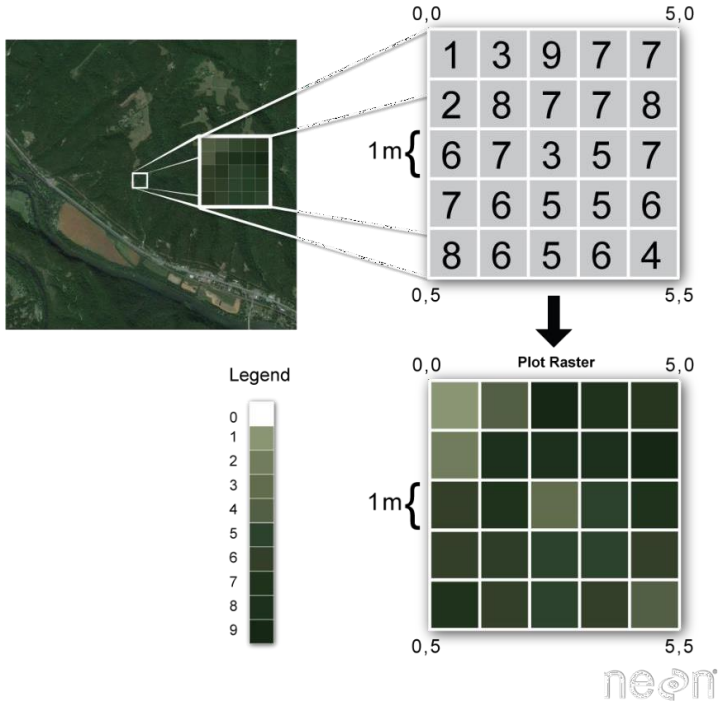

Figure 8. Pixel (Source: https://geohackweek.github.io/raster/02-rasterconcepts/)

One of the most common approaches is the division into grid cells, in which the area is discretised using a regular grid, generally with square cells (Figure 9). Each cell is assigned a numerical value representing the value of a specific variable or influencing factor (e.g. slope, aspect, lithology or land use). This approach is particularly used when input data are available in raster format, as is the case with digital terrain models (DTMs or DEMs) and derived analyses. The main limitation of the grid cell approach lies in its inability to accurately represent the continuous boundaries of natural features such as geological contacts, geomorphological units or catchment boundaries, especially when the size of the

The resolution of the grid cells exceeds the level of detail of the objects represented. Furthermore, the choice of the grid's spatial resolution directly affects both the model's descriptive power and the computational costs of the analysis.

A second approach is represented by Terrain Units, defined on the basis of the distinction between geomorphological, geological and morphostructural characteristics. These units are characterised by a high degree of homogeneity in terms of landform, outcrop materials and dominant morphogenetic processes. This criterion allows for a more realistic representation of the natural conditions of the territory; however, it involves a certain degree of subjectivity in the delineation of the units, linked to the operator's interpretation. A further limitation is the possible coexistence, within the same unit, of multiple active geomorphological processes, which sometimes makes it complex to attribute a univocal behaviour in terms of susceptibility.

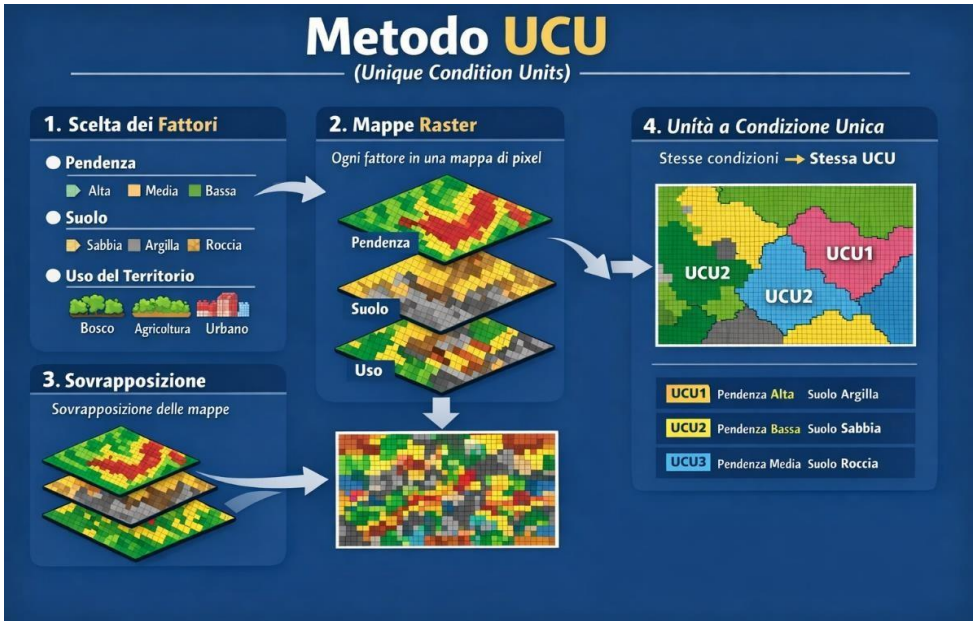

Figure S. UCU method

Unique-Condition Units (UCUs) constitute a classification criterion based on the spatial overlap of thematic maps relating to all the geological and environmental factors considered relevant to the triggering of landslides. Each factor is initially subdivided into a finite number of homogeneous classes; the intersection of the boundaries of these classes generates spatial units characterised by a unique and non-repeatable combination of environmental conditions. Each UCU therefore represents a specific geological-environmental configuration, to which a certain degree of susceptibility may be associated. This approach is particularly suitable when using vector data and is easily implemented using GIS tools, which allow for rapid and efficient management of overlay operations. However, the high number of factors and classes considered can lead to excessive fragmentation of the territory, resulting in an increase in the model's complexity.

A further criterion for classification is based on hydrological or hydrogeological units, the boundaries of which are defined by the drainage network and watershed lines. In this case, catchments and sub-catchments represent spatial units within which morphometric and hydrological parameters (such as drained area, average slope, and topographic convergence index) can be considered predisposing factors for instability. This type of classification is widely used in the literature (Guzzetti et al., 2006a; Coelho-Netto et al., 2007; Rossi et al., 2010), since the geomorphological processes affecting a slope can reasonably be considered homogeneous within a single hydrological unit. The approach can be further refined by integrating lithological, structural or land-use information, thereby improving the representativeness of the defined units.

In some cases, particularly in regional or national-scale studies, political-administrative units—such as cadastral parcels, municipal, provincial or regional boundaries—are adopted as mapping units. This choice is primarily driven by operational requirements, spatial planning needs or the

administrative management of results.

Although in several cases administrative boundaries may coincide with physiographic or geographical limits, in most situations this criterion is not very representative of natural geomorphological processes and therefore constitutes an intrinsic limitation for susceptibility analysis.

The choice of map unit type depends entirely on the analytical method used, the working scale, the type of instability under study, and the nature, resolution and quality of the available data. A correct definition of the map units is a crucial step in ensuring the consistency of the model and the reliability of the susceptibility maps produced.

2.4 Relevant legislation

The complex geological structure of the peninsula, its marked morphological variability and the frequent interaction between natural processes and human activities make landslides a particularly significant issue at national level, including in terms of land safety and planning. For these reasons, the management of such phenomena constitutes an area of specific regulatory focus, falling within the broader framework of soil protection and hydrogeological risk prevention (ISPRA, 2015).

2.4.1 Legislative Decree 152/2006

The main legislative reference is Legislative Decree No. 152 of 3 April 2006 (Consolidated Law on Environmental Provisions), which provides the regulatory framework within which policies for the planning and mitigation of landslide risk are situated.

The Consolidated Act incorporates and reorganises the principles already introduced by Law No. 183 of 18 May 1989, which had recognised hydrogeological instability and landslides in particular – for the first time as phenomena to be addressed through integrated and preventive planning. From this perspective, landslides are considered phenomena of instability closely linked to land use and anthropogenic changes to the territory, moving beyond an exclusively emergency-based approach.

In particular, Part III of the Consolidated Act regulates soil protection as a coordinated set of actions aimed at preventing and reducing the risks arising from geomorphological and hydrological processes, explicitly including phenomena of slope instability.

The river basin is commonly taken as the reference territorial unit in soil protection planning, as it allows landslide phenomena to be analysed from a perspective based on geomorphological and hydrological processes, rather than on administrative boundaries. Within this framework, the District Basin Authorities are responsible for planning and coordinating landslide risk mitigation measures through the development of District Basin Plans and their associated detailed plans. This institutional approach allows the problem of landslides to be addressed in an integrated manner,

taking into account the relationships between slope instability, the dynamics of surface and groundwater, and erosion processes (District Basin Authority, 2016).

However, the use of administrative boundaries in spatial analyses can entail certain limitations, as these boundaries do not always correspond to the actual extent of the geomorphological and hydrological processes that influence slope stability. This can result in an incomplete representation of natural dynamics, sometimes excluding areas that contribute to the hydrological and sedimentary processes of the area under analysis. Despite these limitations, the use of administrative boundaries is often necessary in studies aimed at spatial planning and risk management, as management policies and decision-making tools are generally organised according to administrative subdivisions. Consequently, landslide susceptibility analysis conducted on an administrative basis represents a compromise between the need to consider the natural processes governing slope instability and the need to produce results applicable to land management and planning. The key instrument for regulating landslide-prone areas is the Hydrogeological Structure Plan (PAI), which forms part of the Basin Plan and is specifically aimed at reducing hydrogeological risk. The PAI provides for the identification, delineation and classification of landslide phenomena, distinguishing between active, quiescent and potential landslides, and assigning each area a geomorphological hazard class, generally divided into four increasing levels (P1–P4)1 Hazard is associated with risk assessment (R1–R4), obtained through the a combination of hazard, vulnerability and exposure of elements present in the territory, such as settlements, infrastructure and productive activities (ISPRA, 2015).

The Technical Implementation Regulations of the PAI provide detailed rules governing permitted interventions in landslide-prone areas, introducing restrictions on building and limitations on land use. In particular, in areas characterised by active landslides or very high hazard (P4), the construction of new buildings and infrastructure is generally prohibited, whilst only interventions to secure and stabilise slopes, aimed at reducing hazard and risk, are permitted. In such contexts, any land-use change is subject to proof of the geological and geomorphological compatibility of the intervention (District Basin Authority, 2016).

The Consolidated Act confers binding force on the PAI (Integrated Landslide Prevention Plan) in relation to municipal urban planning instruments, imposing an obligation to incorporate the boundaries of landslide-prone areas and the relevant regulatory requirements. It follows that local urban planning must necessarily take account of the presence of landslide-prone areas, integrating

[1] The Hydrogeological Risk Plans (PAI) use a hazard classification for the entire national territory divided into five classes: very high hazard (P4), high hazard (P3), medium hazard (P2), moderate hazard (P1) and areas requiring attention (AA) (Decree-Law 180/1998 and Prime Ministerial Decree

geomorphological information into the formulation of territorial development plans. The Regions, within the scope of their legislative powers, further regulate the matter through regional laws that define criteria and methodologies for the preparation of landslide hazard studies and the authorisation procedures for interventions in unstable areas.

2.4.2 Other regulatory instruments

The Technical Standards for Construction also play a significant role in the regulatory management of landslides, as they make it mandatory to carry out geological and geotechnical characterisation of sites affected by construction works, with particular reference to areas prone to slope instability (MIT, 2018). In this context, the geological report is a fundamental tool for assessing the stability of slopes and for designing any necessary stabilisation works, thereby contributing directly to the prevention of landslide risk.

Landslide management also encompasses the aspects of residual risk and emergency response. Legislative Decree No. 1 of 2 January 2018, containing the Civil Protection Code, classifies landslides among the main natural risks of geological origin and regulates activities relating to forecasting, monitoring and emergency management. This legislation complements the planning approach of the Consolidated Environmental Act, strengthening the link between knowledge of landslide phenomena, spatial planning and the protection of the exposed population (Legislative Decree 1/2018; Presidency of the Council of Ministers, 2015).

Further technical guidance is provided by the National Environmental Protection System (SNPA) guidelines for landslide monitoring, which offer operational guidance on the design and management of geotechnical, geodetic and meteorological monitoring networks. These guidelines aim to standardise procedures at national level and improve the quality of information available for the management of landslide phenomena (SNPA, 2021). In the technical-scientific field, further

Guidance is provided by the guidelines for landslide risk mitigation drawn up by ISPRA and by technical and scientific associations, such as the Italian Geotechnical Association, which offer design criteria for slope stabilisation works.

2.5 Databases

Alongside the regulatory framework, landslide risk management is based on a comprehensive system of technical tools that enable these phenomena to be quantified, mapped and monitored in a scientifically sound manner. Among these, a central role is played by the Inventory of Landslide Phenomena in Italy (IFFI), compiled and updated by ISPRA in collaboration with the Regions and Autonomous Provinces. The IFFI constitutes the national reference database on landslide phenomena, providing standardised information on the spatial distribution, type of movement and

activity status of landslides, and is widely used for hazard analysis, spatial planning and civil protection activities (ISPRA, 2021).

Information tools such as the IdroGEO platform expand the operational use of IFFI data, making landslide maps and risk indicators available in an interoperable format to public authorities, professionals and civil protection operators. These tools support the implementation of current legislation, facilitating decision-making and the planning of risk mitigation measures.

3. THE CASE STUDY OF THE MUNICIPALITY OF GENOA

The author's internship at ARPAL, the Regional Agency for Environmental Protection of Liguria, led to the research and preparation of data relating to factors predisposing landslides, based on the study conducted by Roccati and Faccini (2021) for the creation of susceptibility maps using the heuristic method of the Analytic Hierarchy Process (AHP)[2] . The topic was subsequently developed during the thesis at the Geomatics Laboratory of the Department of Civil, Chemical and Environmental Engineering at the University of Genoa, testing the SALSA.1 procedure described above on the same area.

3.1 Geographical context

Genoa is a coastal city and the capital of Liguria, situated in north-western Italy, at the northernmost tip of the western Mediterranean. The municipality of Genoa covers an area of approximately 240 km^2, spread mainly along a narrow coastal strip about 30 km long and, to a lesser extent, along the main valley axes of the Bisagno and Polcevera rivers (Paliaga et al., 2019). These watercourses, running predominantly perpendicular to the coastline, define the morphological amphitheatre within which the historic centre and the port area have developed; these have historically represented the hub of urban settlements, industrial activities and transport infrastructure (Paliaga et al., 2018). The distribution of the population is highly uneven, with very high densities in the central areas of the municipality, particularly in the terminal section of the Bisagno floodplain, in the historic amphitheatre near the port and at the mouth of the Polcevera, where figures locally exceed 25,000 inhabitants/km^2 in areas characterised by high flood risk (Paliaga et al., 2019). From a morphological perspective, the municipal territory is bounded by steep Apennine hills, with altitudes ranging from sea level up to a maximum of 1,183 m a.s.l. in the western sector(Monte Reixa) and 989 m above sea level in the eastern sector (Monte Alpesisa), with an average elevation of approximately 279 m above sea level (Paliaga et al., 2018).

[2] Among the heuristic approaches most commonly used in the literature for this type of study, the AHP is in fact a multi-criteria analysis technique widely employed in the field of natural risk management, thanks to its ability to integrate and correlate diverse environmental variables.The method is based on a system of pairwise comparisons organised into matrices, which allows the relative contribution of the various environmental factors involved in triggering landslide phenomena to be assessed and compared. These factors generally exhibit marked spatial and temporal variability, making it necessary to use analytical tools capable of managing such complexity.Within the AHP framework, the factors under consideration are compared with one another using a pairwise comparison matrix, in which the relative importance of each factor compared to the others is expressed using the so-called Thomas fundamental scale
L. Saaty, which generally ranges from 1 to 9 and allows the degree of preference between two criteria to be quantified. Based on this matrix, the relative weights of the various factors are then calculated through a normalisation process, which yields a priority vector representing the importance of each parameter within the model. Finally, the consistency of the judgements expressed is verified using the Consistency Index and Consistency Ratio, in order to ensure the reliability of the comparison matrix.

The gradients are generally steep, with average values exceeding 45% (27°) and widespread areas where they exceed 50% (37°), particularly in the eastern and western parts of the municipality, due to the distance from the coastline and the nature of the exposed rock formations (Faccini, Luino, Sacchini, et al., 2015; Faccini, Luino, Sacchini, Turconi, 2015b; Faccini et al., 2016).

The morphometric structure of the catchment basins, characterised by small surface areas, steep gradients and a well-developed hierarchical drainage network, with numerous first-order watercourses according to Strahler, results in very short concentration times, sometimes less than 30 minutes, favouring flash floods and rapid hydrological responses to intense rainfall events (Paliaga et al., 2019).

The geological characteristics of the Genoa area contribute significantly to the high instability of the slopes. The eastern part of the municipality consists mainly of sedimentary formations, in particular calcareous-marly, clayey and silty flysch, whilst the western part is dominated by ophiolitic complexes, comprising serpentinites and calcareous schists; the central sector has a particularly complex geological configuration, characterised by alternating layers of clayey and silty flysch, basalts and dolomites (GeoPortal of Genoa Municipality)

During their evolution, the rock formations have been subjected to numerous deformational events, both ductile and brittle in nature, linked to Alpine and Apennine orogenic processes, which have resulted in pervasive fracturing of the rock mass and marked heterogeneity in terms of strength and deformability (Paliaga et al., 2019). This structural configuration, together with lithological variability, influences the geotechnical behaviour of slopes and the formation of debris cover and soils with different characteristics, predisposing the triggering of surface landslides and debris flows during heavy rainfall events (Paliaga et al. 2025).

3.2 Climatic aspects

The territory of the municipality of Genoa is characterised by a Mediterranean climate with mild winters and hot summers, and a markedly seasonal rainfall pattern, with average annual rainfall of around 1300 mm concentrated mainly in the autumn months.

The interaction with an open, deep sea basin, the south-facing aspect and the presence of the Ligurian Apennines – which act as an orographic barrier against northerly winds – result in a climate for the coastal area and the central urban amphitheatre characterised by mild temperatures and a limited daily temperature range, abundant rainfall, high levels of solar radiation and constant ventilation.

The inland areas, developed along the valley axes penetrating the Apennine hinterland, exhibit significant microclimatic variations, generally with temperatures a few degrees lower than on the coast, due to the rugged terrain and greater distance from the sea's thermoregulatory effect.

The territory is therefore characterised by a climatically: the relative homogeneity of the coastal strip is contrasted by veritable ‘climatic islands’ inland, determined by specific exposures or different altitudes.

The coldest month is January, with average minimum temperatures of 6.4 °C, maximum temperatures of 11.5 °C and a monthly average of 8.8 °C; the warmest month is August, with figures of 21.4 °C (minimum), 27.2 °C (maximum) and 24.3 °C (average) respectively. A distinctive feature of the local climate is the limited temperature range, both daily and annually: the average difference between the daily minimum and maximum is just over 5 °C, whilst the difference between the average temperature in January and that in August is approximately 16 °C. The minimum temperature recorded on average at least once a year is –2 °C, with an average of three days a year with sub-zero temperatures, although winters characterised entirely by above-zero temperatures are not uncommon. The maximum temperature recorded on average at least once a year reaches 32 °C.

Precipitation is a key factor in determining the local climate. Although Genoa’s average annual rainfall totals and monthly distribution are consistent with a Mediterranean climate, it is characterised by frequent thunderstorms of exceptional intensity, marked by high rates of rainfall over short periods of time. In the event of intense but brief downpours, localised flooding may occur; if rainfall persists for several hours, the effects can take on a flood-like character, as happened in October 1970 and October 2010. The average annual rainfall is 1,296 mm. The rainiest month is October, with an average of 222 mm, whilst July is the driest, with 27 mm, in line with the autumn-winter maximum and summer minimum typical of the Mediterranean climate zone. There are on average 80 rainy days a year, with peaks in autumn and spring (around 9 days a month) and a low in July (3 days). Among the most significant rainfall events is the figure of 948 mm in 24 hours recorded by the Bolzaneto station during the October 1970 flood, a European record for a city; among the intense short-duration episodes, the 123 mm/h in October 1977 and the 396 mm in 6 hours on 4 October 2010 recorded by the ‘Santuario Monte Gazzo’ rain gauge station (Municipality of Genoa, n.d.) are worth noting (figure10).

On average, there are three or four episodes of hail during the year, whilst snowfall is rarer and mainly affects inland and hilly areas. Despite the relatively mild winter climate, the phenomenon known as the ‘dark north wind’ can bring significant snowfall, with accumulations in the inland valleys exceeding 30 cm, though these are generally less substantial in the town centre. Snow generally does not remain on the ground for long: rising temperatures cause it to melt within one or two days, sometimes even within a few hours.

Average wind speeds are around 2.5 m/s, contributing to the city being moderately windy. Relative humidity is lower during the winter months, whilst June is on average the wettest month. Annual

rainfall falls within the typical parameters of the Mediterranean climate; however, between September and November, there have been, over the years, episodes of storms of high intensity and duration, responsible for flooding in various urban areas (Municipality of Genoa, n.d.).

TEMPERATURE	Minime Medie (°C)	Massime Medie (°C)	Media (°C)
gen	6,4	11,5	8,8
feb	6,7	12,1	9,2
mar	9,0	14,3	11,5
apr	11,1	16,4	13,7
mag	14,9	20,3	17,7
giu	18,1	23,5	21,0
lug	21,2	26,8	24,1
ago	21,4	27,2	24,3
set	18,4	24,1	21,1
ott	14,5	19,9	16,9
nov	10,1	15,0	12,3
dic	7,6	12,4	9,8
MEDIA	13,3	18,6	15,9

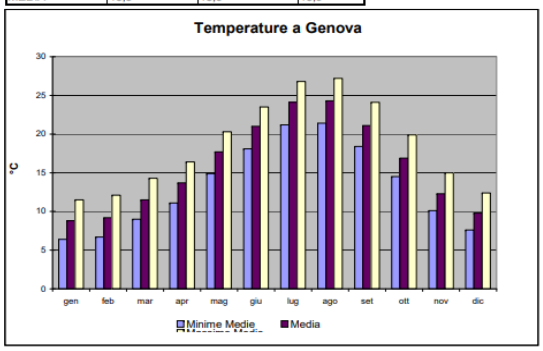

PRECIPITAZIONI	Millimetri / mese	Giorni Piovosi
gen	141	8
feb	76	5
mar	109	7
apr	96	9
mag	78	8
giu	60	5
lug	27	3
ago	85	5
set	139	6
ott	222	9
nov	143	8
dic	120	7
SOMMA	1296	80

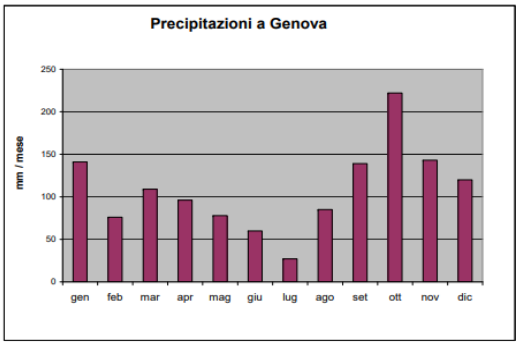

Figure 10: Temperature and rainfall data for Genoa (Source: https://www2.comune.genova.it/sites/default/files/DEF/1_DF/1_01_doc.pdf)

3.3 The effects of climate change in Genoa

Climate analyses conducted in the Genoa area indicate an increase in the average annual air temperature and a reduction in the total number of rainy days, though these are associated with an increase in the intensity of rainfall. This pattern is consistent with a rainfall regime characterised by a greater concentration of cumulative rainfall over short time intervals, resulting in an increase in the frequency and severity of extreme events, which are responsible for more frequent floods and landslides. Furthermore, indicators of extreme rainfall events show a statistically significant upward trend over the period 1979–2019 (Paliaga et al., 2019).

The combination of steep rainfall gradients, small catchment areas and very short run-off times favours rapid hydrological responses, with marked increases in peak discharge and the exceeding of the flow capacity of urban watercourses.

At the same time, the steep slopes, the presence of surface debris cover and widespread human development contribute to the triggering of surface landslides and, in some cases, debris flows, with serious socio-economic impacts (CNR-IRPI; Legambiente, 2021).

According to historical analyses by CNR-IRPI, Genoa is the Italian municipality with the highest number of significant hydrogeological events recorded over the last century (the data cited refer to the period 1889–1999): five significant landslides and six major floods, resulting in a total of 78 fatalities, of which 31 were associated with landslides and 47 with flooding (CNR-IRPI; The Province

of Varese). These figures highlight a combination of high natural hazard — linked to the steep topography of the Ligurian basins and the meteorological dynamics of the Ligurian Sea — and significant human exposure, with urbanisation historically concentrated in the valley floor and along the river courses.

The decision to use administrative boundaries rather than natural ones is motivated by the need to ensure more effective spatial planning management. At the same time, in order to take greater account of the geomorphological and hydrological processes that influence landslide susceptibility, the analysis was conducted across several study areas with different boundaries, comparing the results obtained at different scales. This approach allows for more reliable and applicable susceptibility estimates, particularly at the municipal level, where planning decisions require concrete and actionable results.

4. STATISTICAL METHODOLOGY FOR ASSESSING LANDSLIDE SUSCEPTIBILITY

The methodology used in this study is a statistical method; specifically, it is based on logistic regression and is applicable to various types of landslide phenomena, namely rapid and slow flows, translational-rotational slides, widespread surface landslides, complex landslides and indeterminate landslides. The objective is to identify and quantify the relationship between the distribution of observed landslides and a set of predisposing factors of a morphological, geological and environmental nature, in order to produce a susceptibility map expressing the probability of landslide occurrence in the analysed area.

4.1 Workflow

The workflow consists of several stages. First, the working region and spatial resolution are defined, and the actual working area is delineated using a mask. Next, the maps relating to the predisposing factors are imported. The raster data is imported and checked for extent and resolution. If these exceed those of the working region, the data is cropped and resampled; if they are lower, the data is deemed unsuitable and discarded. The vector data is imported and rasterised.

The imported maps are organised into discrete classes. In particular, for continuous maps (e.g. slope, elevation, etc.), the continuous values are grouped into a number of arbitrary classes. The next step involves preparing the statistical sample based on IFFI landslides, which can be carried out in three different ways: using the entire set of landslides, identifying a percentage of landslides for calibration and the remainder for validation, or selecting a percentage of landslide pixels for calibration and the remainder for validation.

This workflow provides a consistent and comprehensive working environment, where the predisposing factors and the pre-processed landslide sample are ready for subsequent bivariate and multivariate statistical analyses.

During the bivariate statistical analysis phase, the map for each predisposing factor is compared cell by cell with the landslide map, counting the cells in each class that are affected by landslides and those not affected by landslide phenomena, producing an output file in.csv. This allows the conditional probability of landslides occurring to be calculated for each class of every factor. In probabilistic terms, the conditional probability represents the probability that a given event will occur given that a specific condition has occurred. It is defined as:

$$P(A \mid B) = \frac{P(A \cap B)}{P(B)}$$

where:

- $P(A \mid B)$ represents the probability that the event A occurs given B ;
- $P(A \cap B)$ represents the probability that the events A and B occur simultaneously;
- $P(B)$ denotes the probability that the condition B occurs.

In the specific case of landslide studies, the event corresponds to the presence of a landslide, whilst the condition represents a cell's membership of a specific class of a predisposing factor. Operationally, the conditional probability is estimated as:

$$P(\text{landslide} \mid \text{class}) = \frac{N_{\text{landslide, class}}}{N_{\text{class}}}$$

where $N_{\text{landslide, class}}$ is the number of cells belonging to the class in which a landslide is present, and N_{class} is the total number of cells belonging to that class. Higher values indicate a greater propensity of the class in question to host landslides.

The classes are numbered by assigning ascending values starting from 1, based on the probability of landslides occurring. The procedure continues with a multivariate statistical analysis based on logistic regression, to simultaneously assess the combined effect of the various predisposing factors. Logistic regression, which belongs to the family of Generalised Linear Models (GLM), is particularly suited to the study of phenomena characterised by a binary dependent variable. The probability of the phenomenon occurring is expressed using the logit function:

$$\text{logit}(p) = \ln\left(\frac{p}{1-p}\right)$$

where p represents the probability of the landslide occurring. The relationship between probability and predisposing factors is therefore:

$$\text{logit}(p) = \beta_0 + \beta_1 x_1 + \beta_2 x_2 + \cdots + \beta_n x_n$$

with β_n predisposing factors and x_n coefficients estimated by the model.

Subsequently, all possible combinations of the available predisposing factors are tested (255 combinations in the case of eight factors) and evaluated according to Akaike's Information Criterion (AIC) to select the most suitable model. Predictive ability is also verified using the Area Under the Curve (AUC) of the ROC curve.

The selected model is used to generate a map of logit values, subsequently transformed into probabilities using the inverse logistic function:

$$p = \frac{1}{1 + e^{-z}}$$

where z is the value estimated by the model. The continuous probability map is then reclassified into qualitative classes and compared with the landslide inventory to produce a final report on the reliability of the classification.

This sequence of steps constitutes the methodological framework adopted for the production of the landslide susceptibility map and forms the analytical basis for the analyses presented in the following sections.

4.2 The role of Geographic Information Systems (GIS)

Computer systems play a fundamental role in the study of landslide susceptibility, as they enable the integration of information from different disciplines, the application of advanced quantitative models, and the production of maps of high scientific and practical value. The use of these tools allows for the systematic analysis of conditions that trigger landslide phenomena and contributes significantly to the understanding and mitigation of slope instability processes (Aleotti & Chowdhury, 1999; Reichenbach et al., 2018).

Through Geographic Information Systems (GIS), it is possible to integrate numerous types of data into a georeferenced environment, including maps related to lithology, geological structure, land cover, the hydrographic network, and anthropogenic factors, as well as climatic and rainfall data (van Westen et al., 2008). The morphology of the terrain is described and processed using morphometric parameters such as slope, aspect, curvature, and other indicators derived from Digital Elevation Models (DEMs). Furthermore, GIS allow for the management and integration of data from various acquisition techniques, including satellite remote sensing, aerial photography, drone surveys, LiDAR data, and radar techniques such as SAR interferometry (InSAR), tools increasingly used for monitoring and analyzing slope instability phenomena (Metternicht et al., 2005; Reichenbach et al., 2018).

Another highly significant aspect concerns the ability to apply statistical models and advanced analysis algorithms within the GIS environment for susceptibility assessment. In particular, it is possible to use bivariate and multivariate statistical approaches, as well as machine learning-based methodologies, which allow for the identification of relationships between landslide distribution and predisposing factors (Yilmaz, 2009; Reichenbach et al., 2018). The reliability of the models can be assessed using specific performance indicators, such as ROC curves and AUC (Area Under the Curve) values, which measure the predictive capability of the analyses performed (Reichenbach et al., 2018).

In addition to the analytical phase, GIS also plays an essential role in the visualization and communication of results. Susceptibility maps can in fact be easily shared, consulted, and updated via digital platforms and

web services, thereby supporting decision-making in land-use planning, risk management, and civil protection processes (Corominas et al., 2014). The creation of landslide susceptibility maps is therefore a highly useful operational tool for identifying areas most exposed to instability and for defining prevention and mitigation strategies. Furthermore, integrating these maps with data from geotechnical and environmental monitoring systems allows for a better understanding of instability processes and the development of increasingly reliable models for risk analysis and management (van Westen et al., 2008; Corominas et al., 2014).

In the field of GIS, numerous software programs are available that enable the management, analysis, and representation of spatial data. These tools can be divided into two main categories: proprietary software and open-source software, which differ primarily in terms of distribution methods, licensing costs, access to source code, and level of flexibility in use (Steiniger & Hunter, 2013).

Among proprietary software, one of the most widely used internationally is ArcGIS, developed by Esri. This platform offers a wide range of tools for spatial analysis, geographic database management, geospatial modeling, and cartographic production. The suite includes various application environments, including desktop tools, web platforms, and solutions for the management and sharing of geospatial data on a large scale. However, the use of proprietary software generally requires the purchase of licenses and can lead to a certain degree of dependence on the manufacturer regarding updates, technical support, and format compatibility (Longley et al., 2015). This situation is commonly referred to as vendor lock-in, that is, a condition in which the user remains tied to a specific software ecosystem.

In recent years, there has been a growing proliferation of open-source GIS software, which represents an increasingly popular alternative in both academic and professional settings. Among these, one of the best known is QGIS, developed by the international QGIS Project community. QGIS enables numerous spatial analysis operations, raster and vector data management, geoprocessing, and cartographic production, as well as integration with various geographic databases (Graser & Olaya, 2015).

The use of open-source software offers several advantages. First, it does not require the payment of licenses, making these tools more accessible to public agencies, academic institutions, and professionals. Furthermore, the open source code allows users to modify and adapt it to their needs, fostering a collaborative approach to the development and improvement of applications (Steiniger & Hunter, 2013). An additional advantage concerns data portability and interoperability, as these software packages generally support numerous standard formats and integrate easily with other geospatial libraries and tools. In the case of QGIS, for example, it is possible to use open-source libraries such as GDAL for managing raster and vector data or GRASS GIS for performing advanced spatial analyses.

Finally, the use of open-source environments promotes the replicability of scientific analyses, an aspect particularly relevant in the research context. The absence of licensing constraints and the ability to share tools and procedures allow other researchers to easily reproduce the results obtained and further develop the

methodologies applied (Longley et al., 2015). For these reasons, open-source GIS software is now an increasingly popular solution for the analysis and management of spatial data, offering a flexible, collaborative, and constantly evolving environment.

4.3 Section on scripts

From a technical perspective, this methodology has been implemented using a series of Python scripts developed for use within the GRASS GIS environment. The scripts are available on GitHub. The approach is optimised for the use of Open Data and requires a set of predisposing factors and landslides listed in the IFFI database.

1) fr_01_impostazioni_W.py: sets up the working environment by configuring the spatial resolution

   and the analysis mask
2) fr_02_importa_DTM_W.py: imports the DTM
3) fr_03_pend_espo_acc_W.py: creates slope, aspect and accumulation maps from the DTM and reclassifies them (using the FAO classification)
4) fr_04_quota_reclass_W.py: reclassifies the DTM into elevation classes
5) fr_05_litologia_W.py: imports the lithology map produced by CNR IRPI
6) fr_06_trasporti_W.py: imports road and rail routes (line vector) and creates buffers of 50, 100, 150 and 200 metres
7) fr_07_ususuolo_W.py: imports a vector map of land use that has already been grouped into broad categories expressed as numbers
8) fr_08_aggr_climatica_W.py: imports the climate aggressiveness map and reclassifies it
9) fr_0999_01_tipi_di_frana_franaW.py: imports the landslides from the inventory of landslide phenomena in

   Italy and categorises them by type
10) fr_0999_02_calibr_valid_frana_W.py: for each type of landslide to which the statistical methodology applies, divides the previously imported dataset into a calibration set and a validation set
11) fr_1000_prob_cond_csv_W.py: creates a folder within the working directory for each type of landslide and, for each factor and for each type of landslide, compares the landslide pixels with the area of each class and saves the results in a .csv file within the relevant folder
12) fr_1001_riordina_classi_W.py: creates a mapset for each type of landslide and, for each type of landslide and for each factor, creates a txt file of rules that assigns an increasing value to the classes based on the conditional probability of a landslide

13) fr_1002_reclassify_factors_W.py: for each type of landslide, reclassifies each factor based on the .txt file created
14) fr_1003_logit_W.py: for each type of landslide, creates a logit map according to the logit formula = ln(p + 0.000000001) - ln(1 - p + 0.000000001), where p = probability of a landslide (i.e. = 1 in landslide-prone areas and 0 in non-landslide-prone areas) and the value 0.000000001 is added to avoid the logarithm of 0
15) fr_1004_COMBOS_W.py, for each type of landslide, relates the various predisposing factors to the logit using logistic regression; considers all possible combinations of factors; uses the Akaike Information Criterion (AIC) to determine which combination of factors yields the model that best fits the data (lowest AIC value); creates the map of expected values corresponding to the chosen model; assesses the reliability of each model on the calibration and validation sets by calculating the Area Under the ROC Curve (AUC) and saves the AIC values for the different combinations as text and CSV files in the working folder
16) fr_1005_susc_univar_W: for each type of landslide, it generates susceptibility maps using the inverse logit formula, compares the resulting susceptibility maps with the landslides in the calibration set, and saves the results as a .csv file (this must be run twice)
17) fr_1006_classi_suscettibilita_W.py: for each type of landslide, reclassifies the susceptibility map into low, medium and high susceptibility classes based on the previously created .csv file
18) fr_1007_report_per_classi_W.py: for each type of landslide, it generates a .txt file showing the percentage of cells affected by landslides for each susceptibility class.

The scripts mentioned are still under development and, as part of the thesis work, have been modified to correct various bugs that emerged during the study.

4.4 Predisposing factors and available data

This study considered the predisposing factors identified by Roccati, A. and Paliaga, G. (2021) and those used to develop the SALSA.1 procedure, as well as the datasets required to include them in the susceptibility calculation. Several factors are common to both procedures, but the datasets used differ.

4.4.1 Hydrology

Proximity to watercourses and springs can contribute to altering local hydrogeological conditions, increasing soil saturation and reducing shear strength, with a consequent increase in susceptibility to the triggering of surface landslides

ARPAL Dataset	Pre-processing	ARPAL Class	SALSA.1 Dataset	Pre-Processing	SALSA.1 Class
Hydrographic Network and Catchments Scale 1:10,000 Year: 2025 Reference System: ETRS89-ETRF2000 / UTM Zone 32N (EPSG:7791)	A 10-meter buffer around springs and watercourses was created to identify an area immediately adjacent to water bodies, potentially subject to significant variations in moisture and pore pressure.	1. Watercourses 2. No watercorses			

Table 1. Description of hydrogeological map

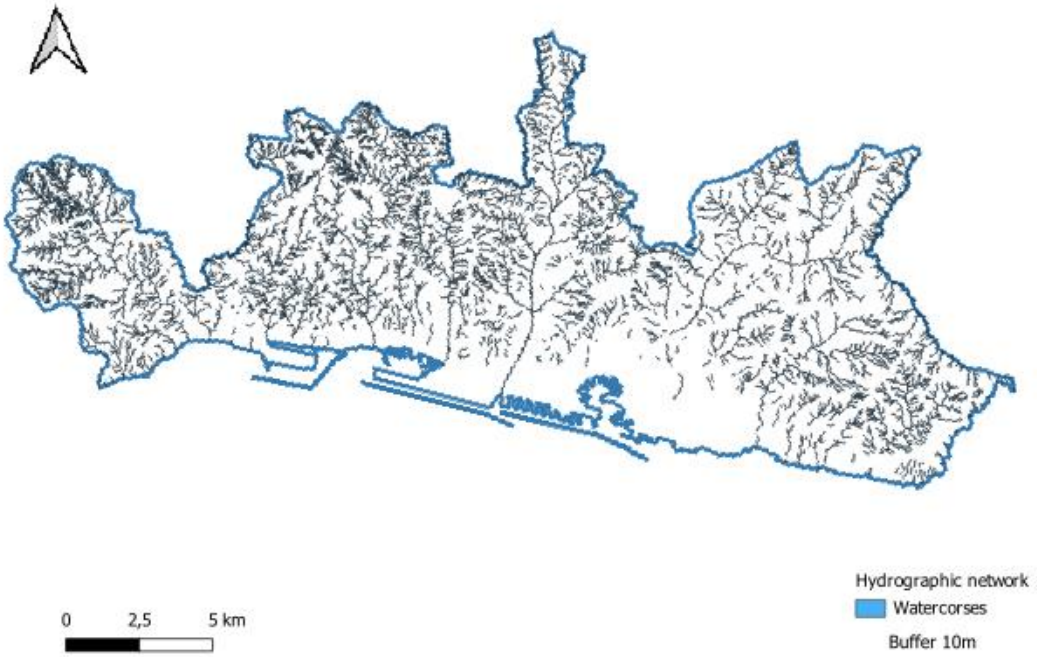

Figure 11. Hydrographic network (buffer zone = 10m): 1. Watercourses; 2. No watercourses

4.4.2 Lithology

Lithological characteristics have a direct and significant influence on slope stability, determining how materials react to natural stresses (such as heavy rainfall, changes in the water regime, surface erosion or seismic activity). In general, compact and cohesive rocks, such as limestone and sandstone, tend to provide greater stability to slopes, whilst such as clays, marls or debris deposits, are more prone to instability and landslides.

ARPAL Dataset	Pre-processing	ARPAL Class	SALSA.1 Dataset	Pre-Processing	SALSA.1 Class
Lithology Scale 1:50000 Year2017 Reference System ETRS89-ETRF2000/UTM32N (EPSG:7791)	The map was modified by replacing the deposits and unconsolidated covers with the corresponding bedrock layer, assuming that it is the same as that found beneath the surrounding areas. The landslide susceptibility of the rock type was also considered; in cases of uncertainty between two rock types, the one with the higher susceptibility was adopted	1 peridotiti 2 metabasiti 3 gabbri e metagabbri 4 diaspri 5 calcare 6 dolomie 7 serpentiniti 8 scisti filladici e porfiroidi 9 flysch calcareo-marnosi 10 conglomerati 11 calcescisti, micascisti e quarzoscisti 12 ardesie 13 argille e marne plioceniche 14 flysch argillitici	The map used is this: https://essd.copernicus.org/articles/14/4129/2022/essd-14-4129-2022.html It can be downloaded here: https://doi.org/10.1594/PANGAEA.935673 (Bucci et al., 2021).		3 depositi alluvionali 6 flysch 12 rocce carbonatiche 13 rocce intrusive 14 rocce non scistose 15 rocce scistose 16 sedimenti clastici cementati 17 sedimenti clastici sciolti 18 serie calcareo silico marnosa 20 spiagge

Table 2.Lithology

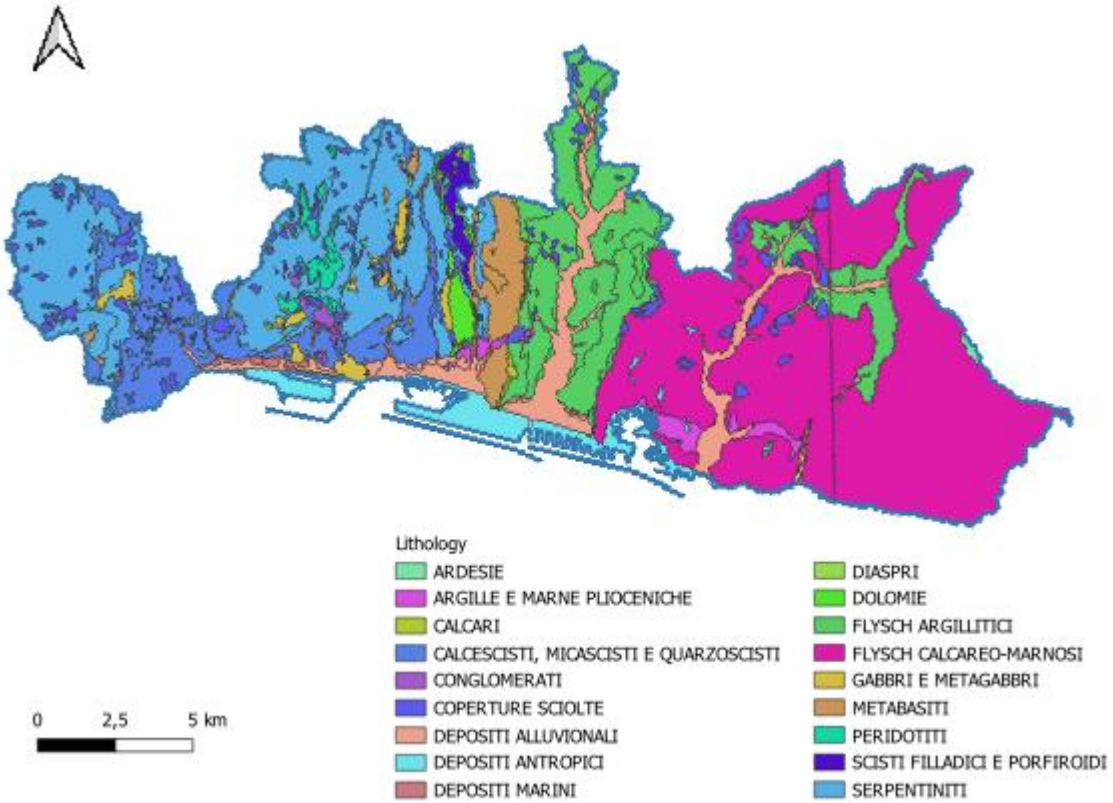

Figure 12. Lithology: 1. Slates; 2. Pliocene clays and marls; 3. Limestones; 4. Calcareous schists, mica schists and quartz schists; 5. Conglomerates; c. Loose cover; 7. Alluvial deposits; 8. Anthropogenic deposits; S. Marine deposits; 10. Jaspers; 11. Dolomites; 12. Clayey flysch; 13. Calcareous-marly flysch; 14. Gabbro and matagabbro; 15. Metabasites; 1c. Peridotites; 17. Phyllitic and porphyroid schists; 18. Serpentinites

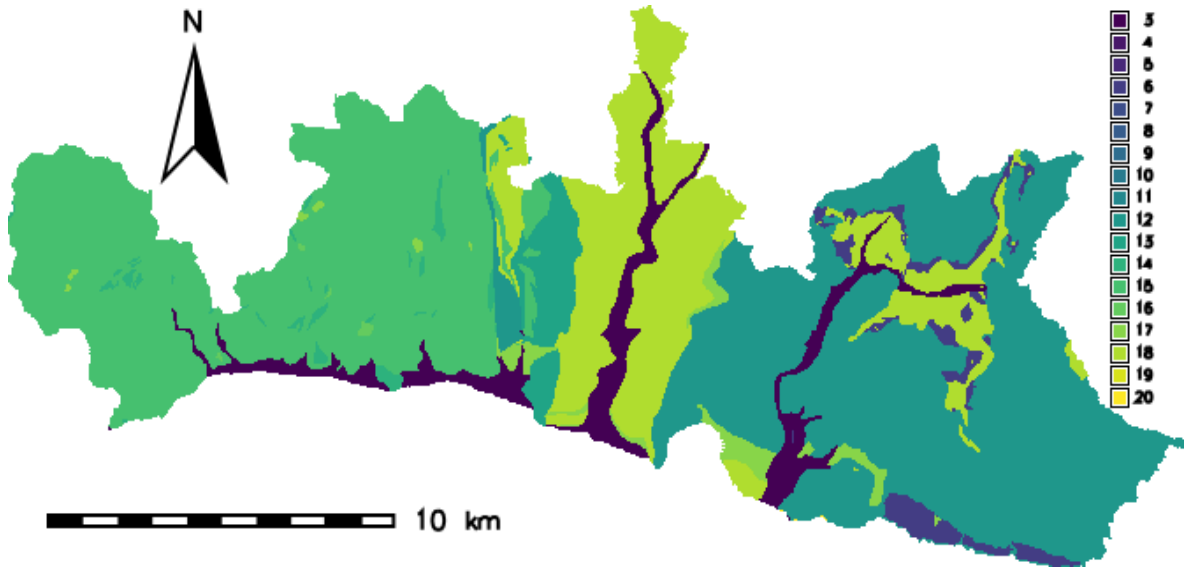

Figure 13. Lithology: 1. 3 alluvial deposits; c flysch; 12 carbonate rocks; 13 intrusive rocks; 14 non-schistose rocks; 15 schistose rocks; 1c cemented clastic sediments; 17 unconsolidated clastic sediments; 18 calcareous-siliceous-marly series; 20 beaches

4.4.3 Elevation

ARPAL Dataset	Pre-processing	ARPAL Class	SALSA.1 Dataset	Pre-Processing	SALSA.1 Class
			Processed from DTM (r.slope.aspect)	The elevations reported in the DTM are grouped into 250 m classes starting from the lowest point of the study area	

Table 3 Description of the elevation map

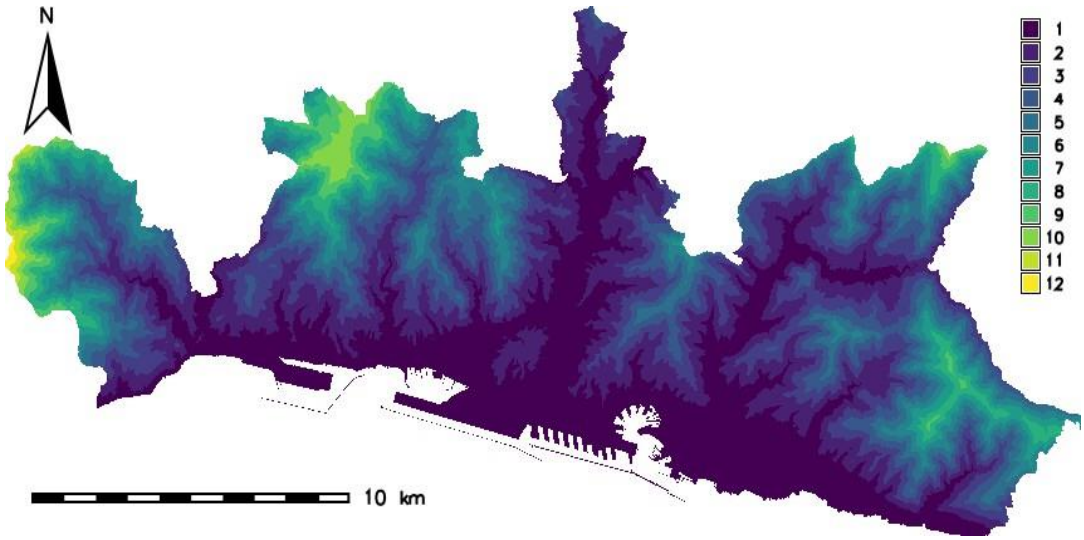

Figure 14. Altimetry

4.4.4 Slope aspect

Slope aspect refers to the orientation of the slope relative to north. For the purposes of this study, it indicates how a slope faces in relation to solar radiation and wind direction, factors that determine microclimatic conditions and soil moisture

ARPAL Dataset	Pre-processing	ARPAL Class	SALSA.1 Dataset	Pre-Processing	SALSA.1 Class
Slope aspect Scale 1:10000 Year2023 Reference System ETRS89- ETRF2000/UTM32 N (EPSG:7791)		North North-east East South-east South South-west West North-west Zenith	Processed from DTM (r.slope.aspect)	Grouping of the values into four classes plus an additional class for flat areas	North (0-45° and 315° 360°) East (45° 135°) South (135° 225°) West (225° 315°) Zenith (0°)

Table 4. Slope aspect

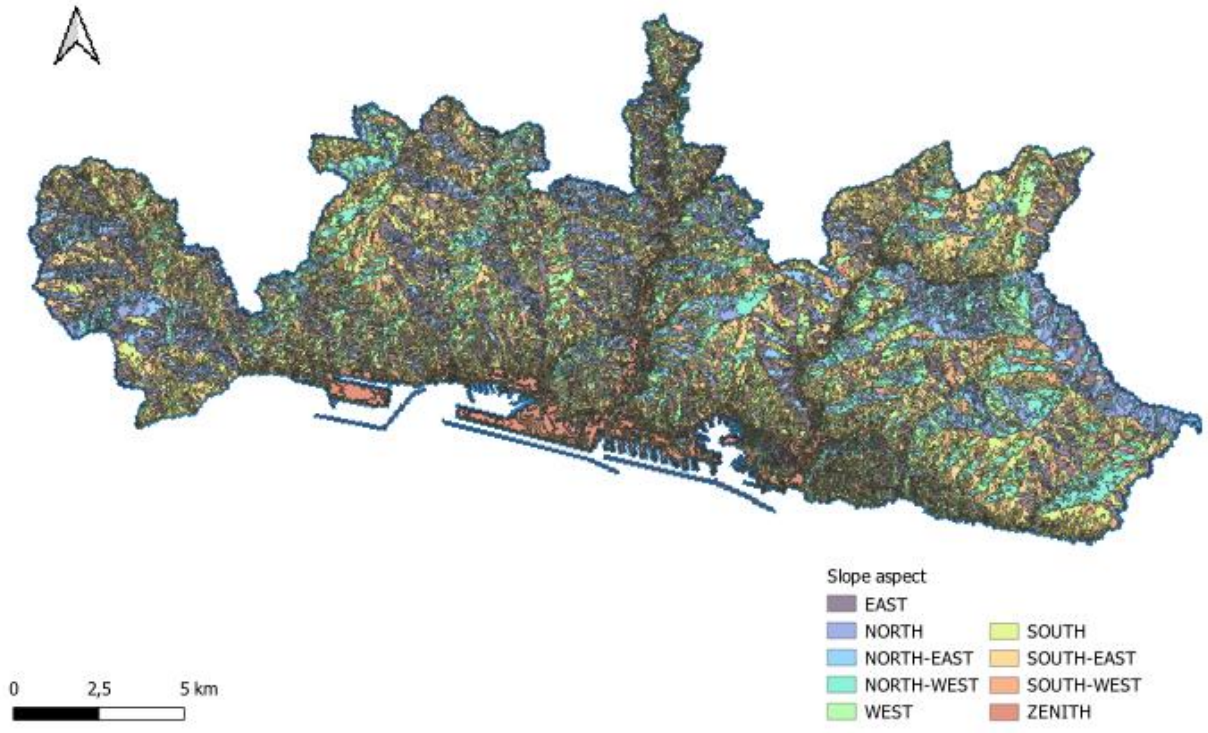

Figure 15. Slope aspect: 1. East; 2. North; 3. North-East; 4. North-West; 5. West; 6. South; 7. South-East; 8. South-West; 9. Zenith

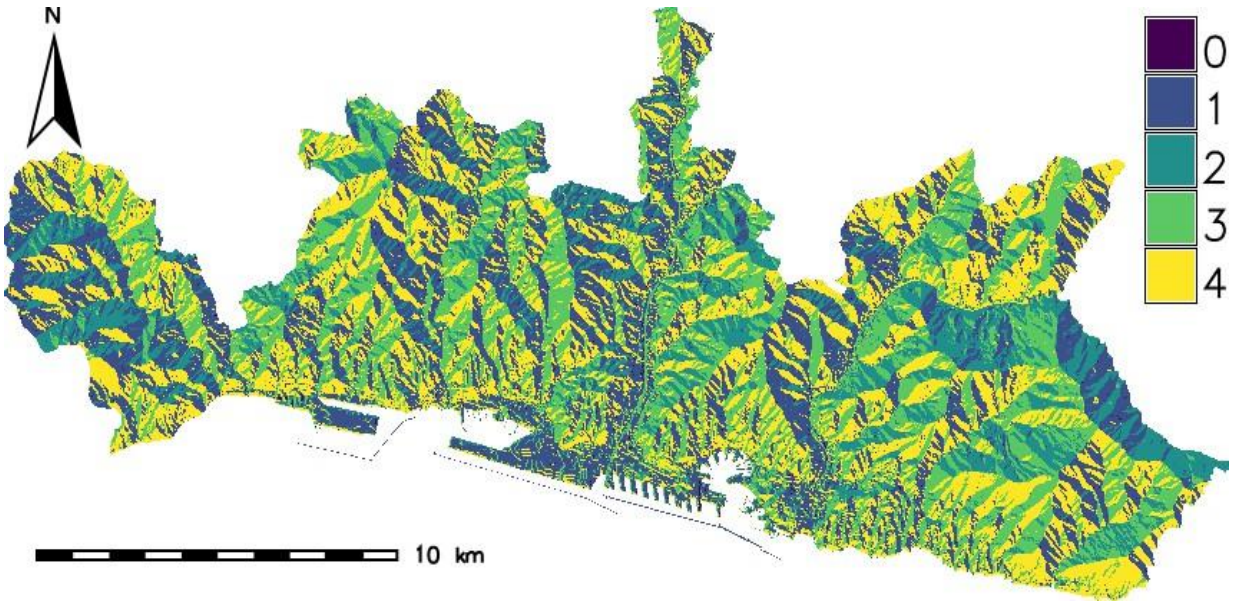

Figure 1c: Aspect; North (0–45° and 315°–360°); East (45°–135°); South (135°–225°); West (225°–315°)

4.4.5 Slope steepness

Slope gradient influences surface degradation processes, the local hydrological regime and the dynamics of potential landslide events. In particular, it affects the erosion coefficient and the infiltration capacity of rainwater, thereby influencing the water balance and the mechanical strength of the soil

ARPAL Dataset	Pre-processing	ARPAL Class	SALSA.1 Dataset	Pre-Processing	SALSA.1 Class
Slope steepness Scale 1:10000 Year2017 Reference System ETRS89- ETRF2000/UTM32 N (EPSG:7791)		1 (0–10%) 2 (11–20%) 3 (21–35%) 4(36–50%) 5 (51–75%) 6 (76–100%) 7 (>100%)	Processed from DTM (r.slope.aspect)		1 (0-5°) 2 (5°-10°) 3 (10°-15°) 4 (15°-20°) 5 (20°-25°) 6 (25°-30°) 7 (30°-35°) 8 (35°-40°) 9 (40°-90°)

Table 5. Slope Map Description

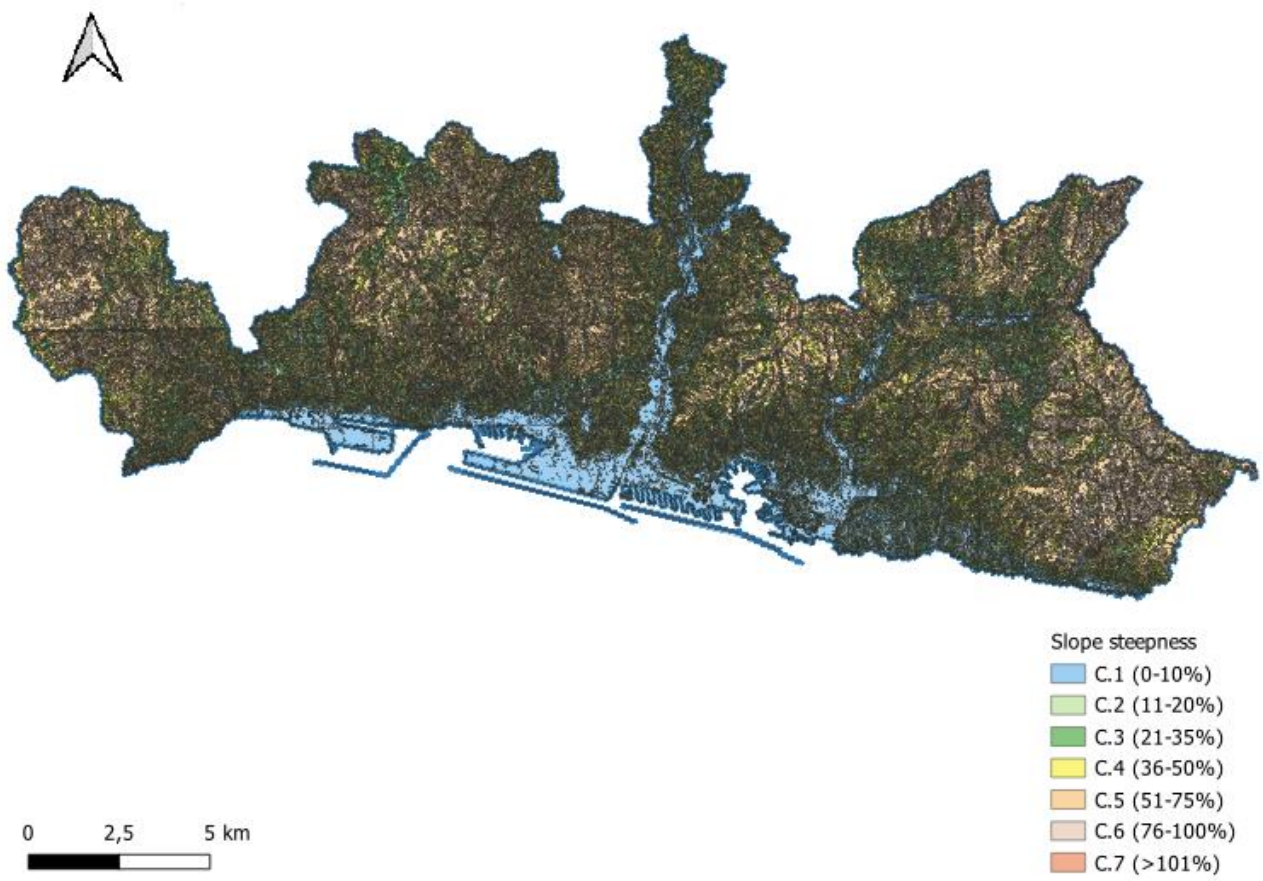

Figure 17. Slope Steepness: 1. 0–10%; 2. 11–20%; 3. 21–35%; 4. 30–50%; 5. 51–75%; 6. 70–100%; 7. >101%

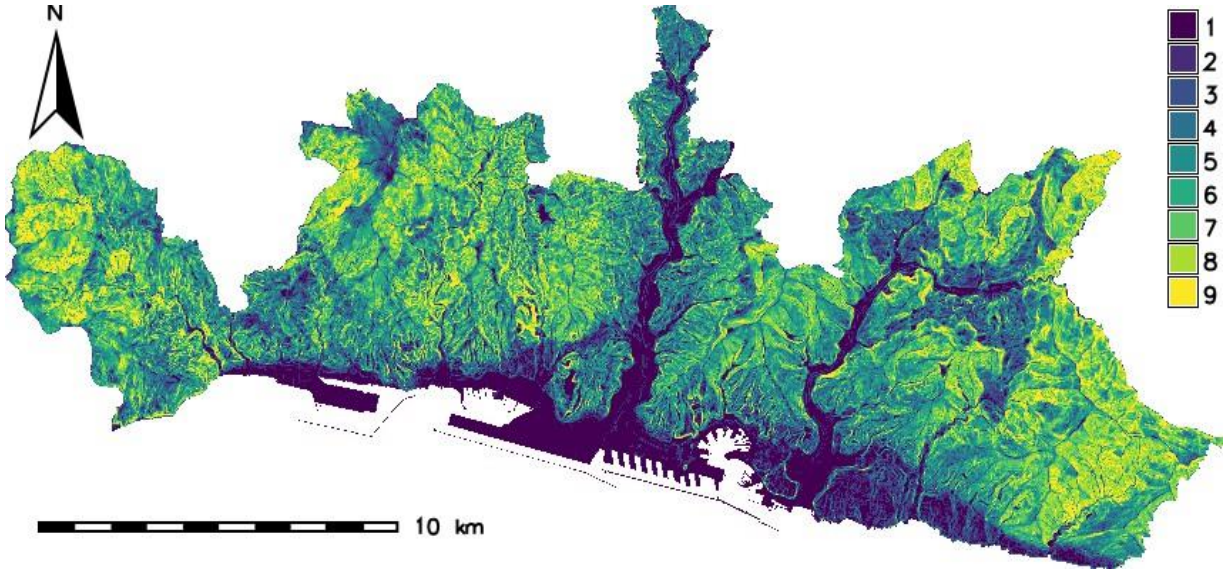

Figure 18: Slope Steepness: 1. 0–5°; 2. 5°–10°; 3. 10°–15°; 4. 15°–20°; 5. 20°–25°; c. 25°–30°; 7. 30°–35°; 8. 35°–40°; S. 40°–S1°

4.4.6 Accumulation

Water accumulation makes it possible to estimate the convergence of surface water flows and an area's capacity to collect or drain rainwater. An increase in soil water content leads to a reduction in the shear strength of materials and an increase in pore pressure, thereby promoting the onset of instability phenomena

ARPAL Dataset	Pre-processing	ARPAL Class	SALSA.1 Dataset	Pre-Processing	SALSA.1 Class
			Processed from DTM (r.slope.aspect)	The accumulation values were normalized using the formula Log(abs|accumulation|) and subsequently classified into six classes.	1 (0-1) 2 (1-2) 3 (2-3) 4 (3-4) 5 (4-5) 6 (5-14)

Table 6. accumulation description

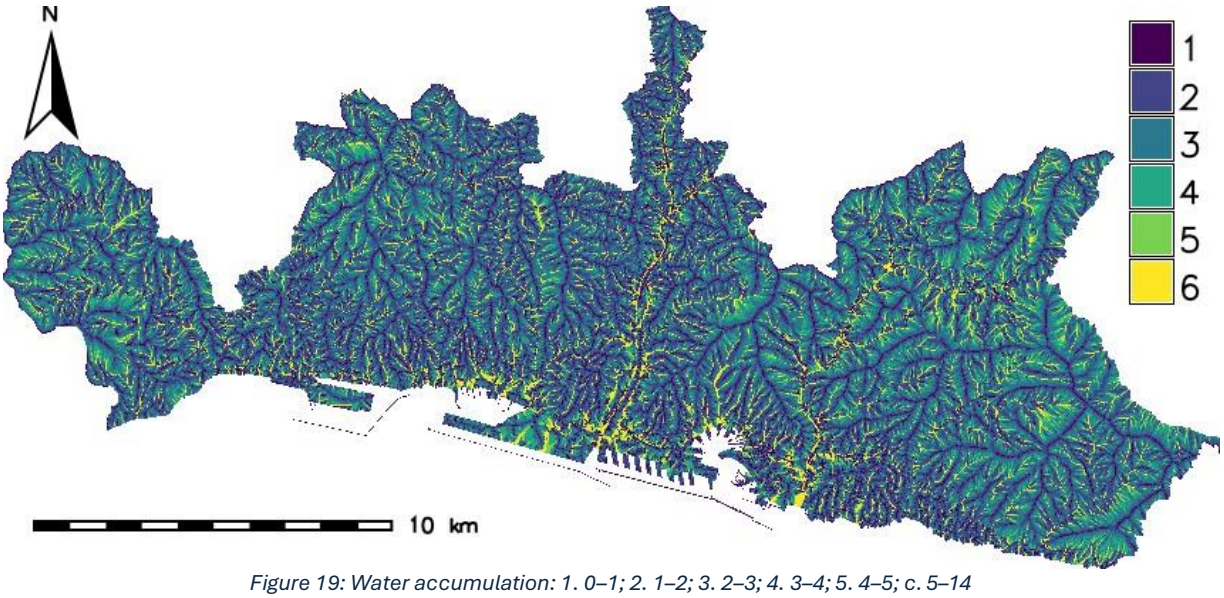

Figure 19: Water accumulation: 1. 0–1; 2. 1–2; 3. 2–3; 4. 3–4; 5. 4–5; c. 5–14

4.4.7 Land Use

Similar to Land Cover, this focuses on 'what' is done in a given area. The land use map is divided into classes based on functional and socio-economic criteria. These identify urban areas, agricultural zones, forests and impervious surfaces, providing useful information for environmental assessments, spatial planning and hydrogeological risk management

ARPAL Dataset	Pre-processing	ARPAL Class	SALSA.1 Dataset	Pre-Processing	SALSA.1 Class
Lande use Scale 1:10000 Year2025 Reference System ETRS89-ETRF2000/UTM32 N (EPSG:7791)	The adopted classification follows level 2 of the CORINE Land Cover (CLC) nomenclature.	Urban fabrics Industrial, commercial and trasport units Mining areas, construction sites, landfills and artificial and abandoned lands Artificial, non-agricultural areas Arable land Permanents crops Heterogeneous agricultural areas Forests Shrubs and/or herbaceous vegetation association Open spaces with little or no vegetation Continental waters Maritime waters			

Table 7. Land use description

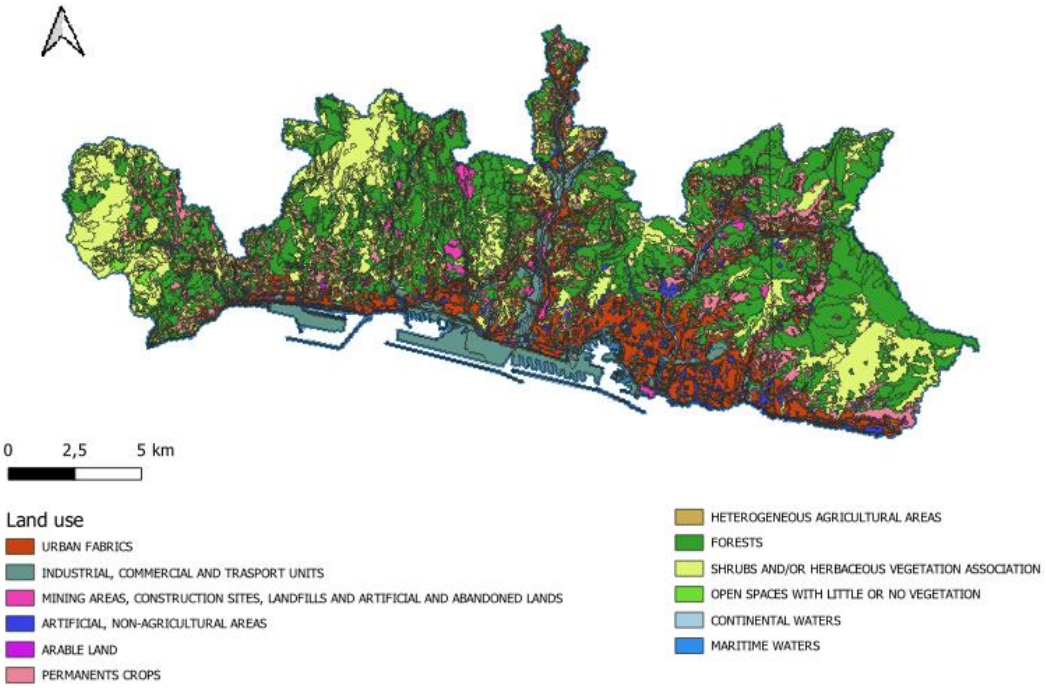

Figure 20. Land use, based on the 2nd level of the CORINE classification (European Environment Agency, 1SS5): 1. Urban areas; 2. Industrial, commercial and transport units; 3. Mining areas, construction sites, landfills and artificial and abandoned land; 4. Artificial, non-agricultural areas; 5. Arable land; 6. Permanent crops; 7. Heterogeneous agricultural areas; 8. Forests; 9. Shrubs and/or herbaceous vegetation; 10. Open spaces with little or no vegetation; 11. Inland waters; 12. Marine waters

4.4.8 Land cover

Similar to Land Use, it focuses on 'what' is found in a given area. Different types of land cover influence soil stability, drainage capacity and surface cohesion

ARPAL Dataset	Pre-processing	ARPAL Class	SALSA.1 Dataset	Pre-Processing	SALSA.1 Class
			Lande use Scale 1:10000 Year2018 Reference System ETRS89-ETRF2000/UTM32N (EPSG:7791)	The dataset was reclassified according to the Land Cover Classification System (LCCS) developed by the FAO (Food and Agriculture Organization)	1 built-up 2 crops 3 tree cover 4 shrubland 5 grassland 6 bare - sparse vegetation 7 water 8 herbaceous wetland

Table 8. Land cover description

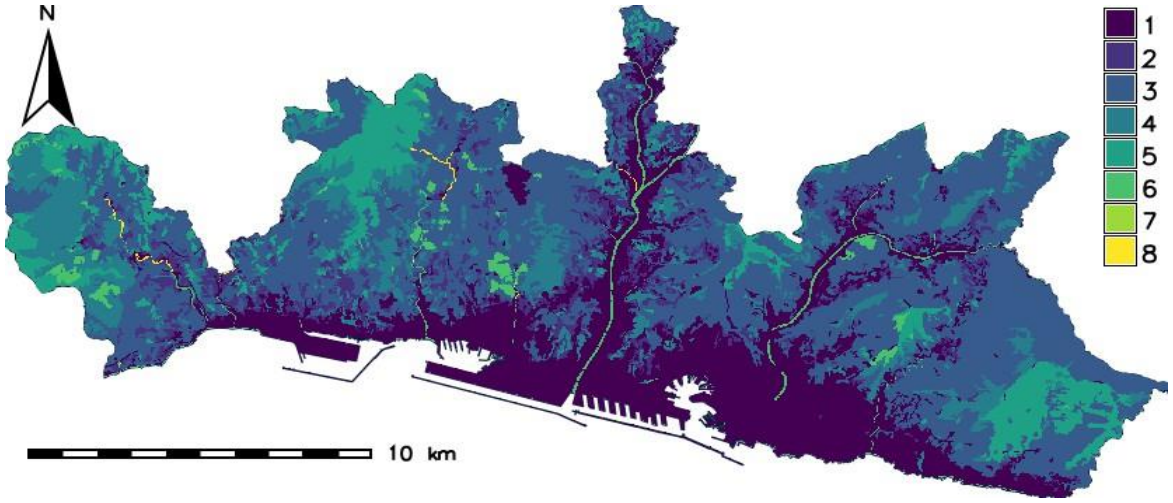

Figure 21. Land use: 1. Built-up: 2. Crops; 3. Tree cover; 4. Shrubland; 5. Grassland; 5. Bare - sparse vegetation; c. Water; 7. Herbaceous wetland

4.4.9 Terraces

According to various scientific studies, actively maintained terraces[3] help to mitigate hydrogeomorphological processes by controlling surface runoff, reducing linear and areal erosion, and increasing the infiltration of rainwater. However, if abandoned, they can lead to a significant loss of efficiency in the hydrological regulation of the slope, increasing susceptibility to landslides during extreme rainfall events.

[3] At the same time, evidence from recent studies suggests that the spontaneous recolonisation of abandoned terraces by shrub and forest vegetation can promote renaturalisation processes, improving soil cohesion and slope stability in the medium to long term. Despite this, surface landslides triggered by heavy rainfall have been documented both in renaturalised terraced areas and in those still under active agricultural management, suggesting that the mere presence of terracing, regardless of its state of maintenance, does not constitute a definitive factor of stability. Based on the study by Roccati et al. (2021) in the municipality of Portofino (Roccati_Faccini; 2021), it was deemed appropriate to include terraced areas among the anthropogenic variables capable of influencing the triggering of landslide phenomena.

ARPAL Dataset	Pre-processing	ARPAL Class	SALSA.1 Dataset	Pre-Processing	SALSA.1 Class
Lande use Scale 1:10000 Year2025 Reference System ETRS89-ETRF2000/UTM32N (EPSG:7791)	It was assumed that areas classified as olive groves, abandoned olive groves, vineyards, abandoned vineyards, and/or other types of permanent crops (non-olive groves), as well as mixed vineyards and olive groves, are terraced	1. Non terraced area 2. Terraced area			

Table 9. Terraces description

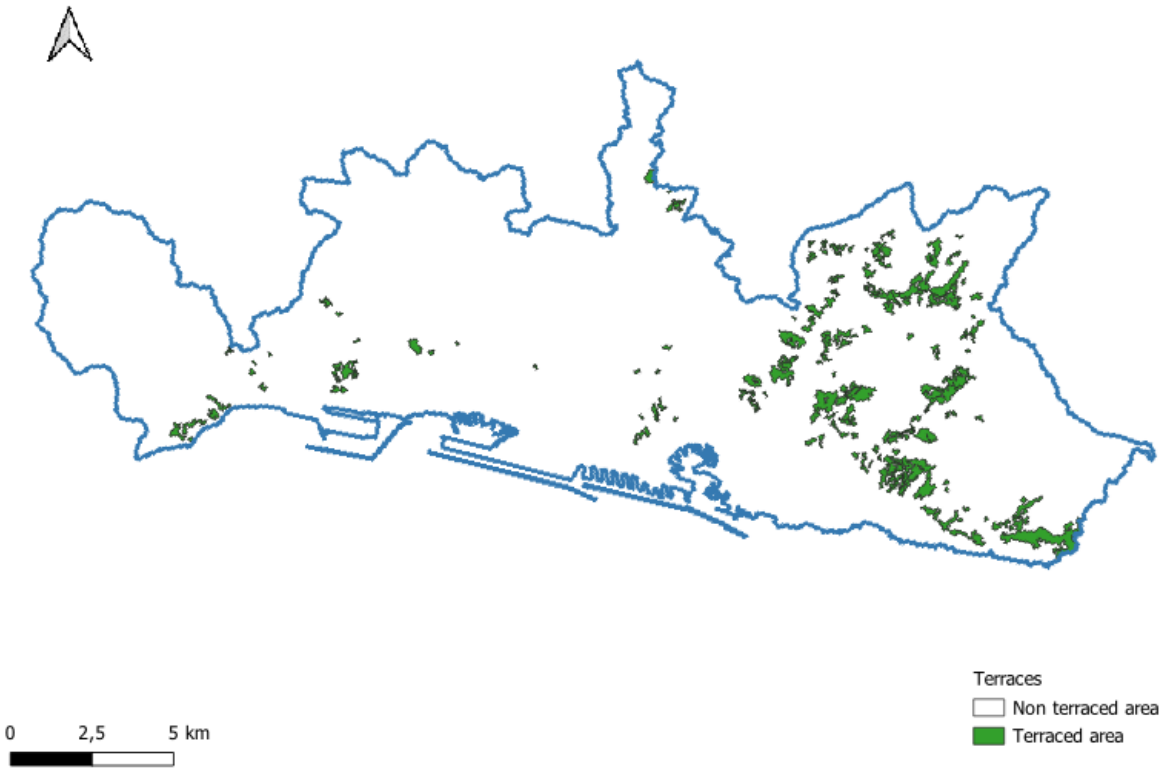

Figure 22. Terraces: 1. Non-terraced area; 2. Terraced area

4.4.10 Man-made cuts

Changes to slopes caused by excavation and backfilling operations for the construction of linear infrastructure (such as roads, footpaths or railways) alter local geotechnical conditions, changing the stress-strain regime. The presence of buildings and associated structures can alter local hydrogeological and mechanical conditions, changing load regimes, surface drainage and infiltration dynamics, with possible effects on the susceptibility to the triggering of surface landslides

ARPAL Dataset	Pre-processing	ARPAL Class	SALSA.1 Dataset	Pre-Processing	SALSA.1 Class
Various regional network Scale 1:5000 Years 2013 Reference System (EPSG:7791) REL-Rete escursioni Liguria Scale 1:25000 years 2025 Reference System (EPSG:7791)	5-meter buffer around the elements	1. Main roads network 2. Rail transport headquarters; 3. Secondary mixed road network; 4. Liguria hiking network: ligurian mountains high route; 5. Liguria hiking network: other routes	Various regional network Scale 1:5000 Years 2013 Reference System (EPSG:7791) REL-Rete escursioni Liguria Scale 1:25000 years 2025 Reference System (EPSG:7791)	For both road and railway routes, tunnel sections and bridges were excluded, as they do not interact directly with the slope morphology. Progressive buffers at distances of 50, 100, 150, and 200 meters were then created from the road and railway routes.	1 Main roads network 3 Rail transport headquarters 3 Secondary mixed road network

Table 10. Man made cuts description

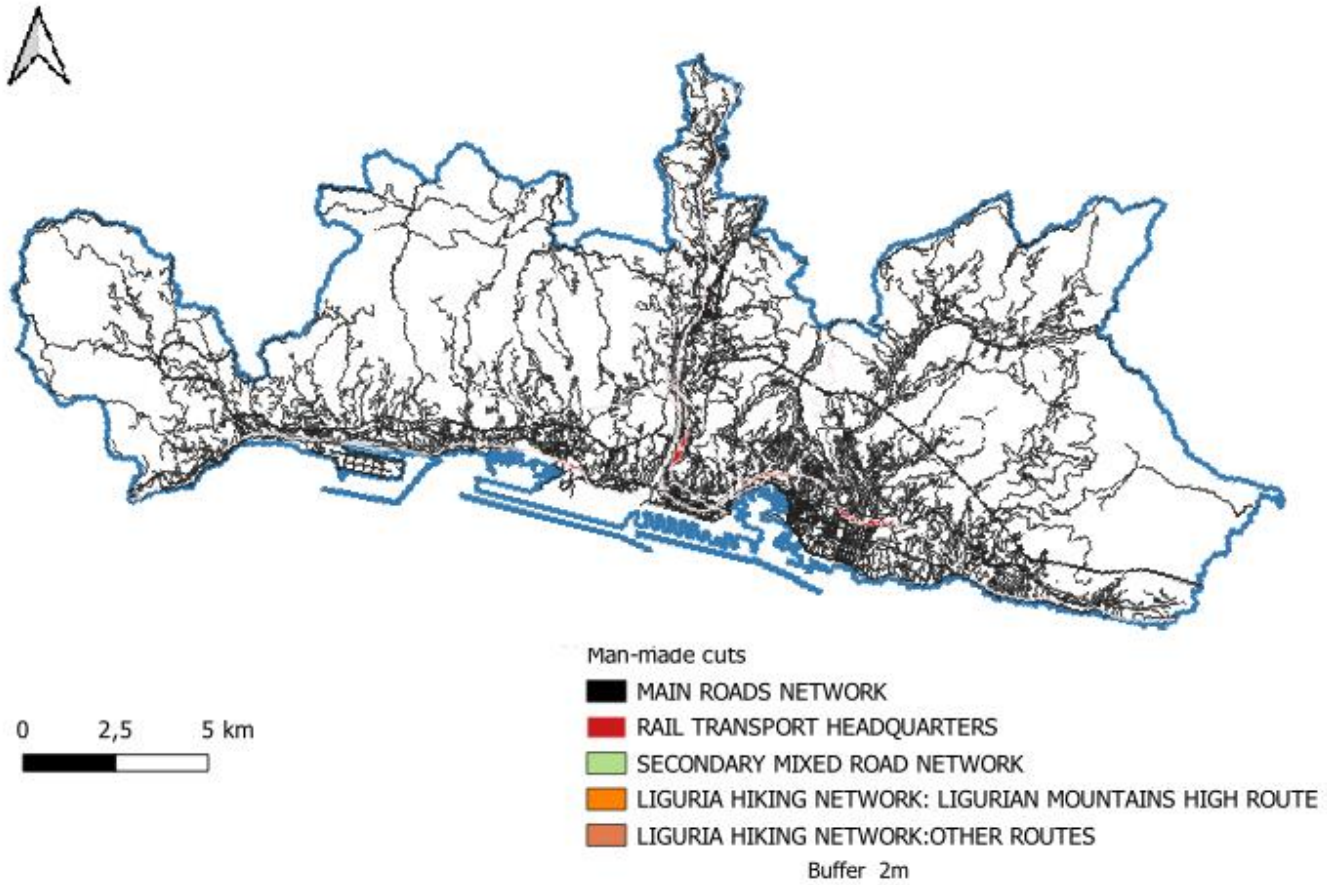

Figure 23. Man-made cuts (buffer zone = 5m): 1. Main road network; 2. Rail transport network; 3. Secondary mixed road network; 4. Liguria hiking network: Ligurian Mountains High Route; 5. Liguria hiking network: other routes

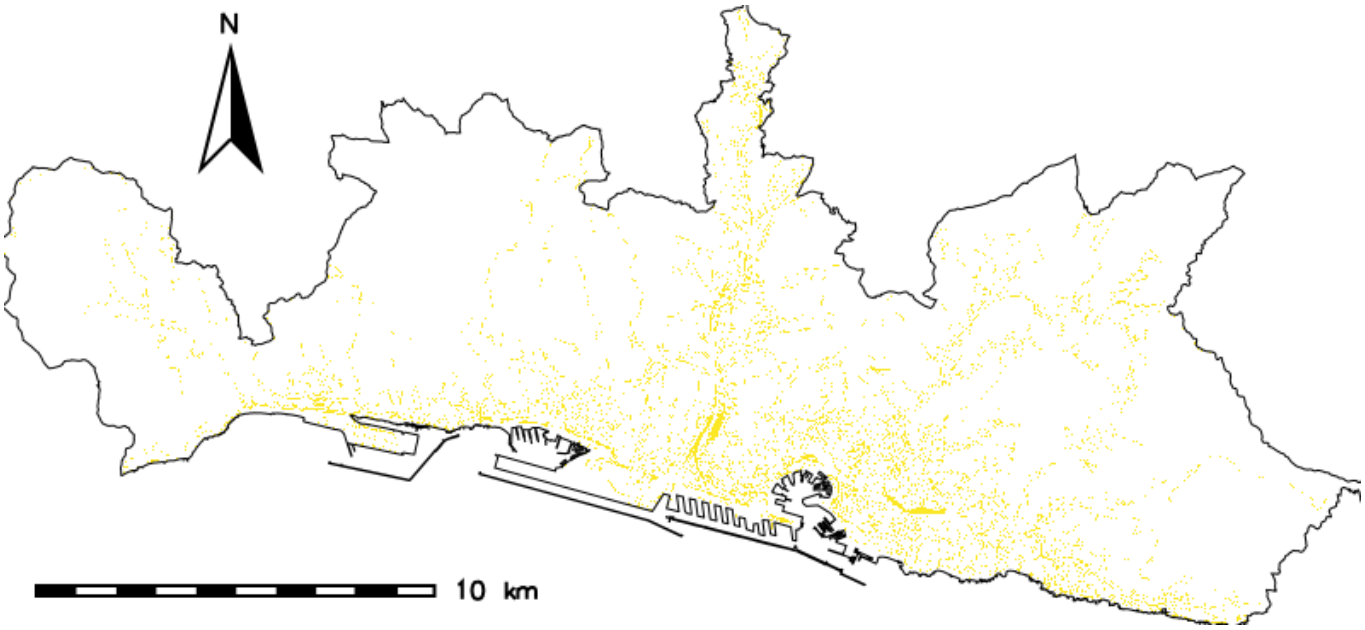

Figure 24. Man-made cuts

4.4.11 Anthropogenic structures

The presence of buildings and associated structures can alter local hydrogeological and mechanical conditions, modifying load regimes, surface drainage and infiltration dynamics, with possible effects on the likelihood of triggering surface landslides.

ARPAL Dataset	Pre-processing	ARPAL Class	SALSA.1 Dataset	Pre-Processing	SALSA.1 Class
Buildings and Manufacts Scale 1:5000 years 2013 Reference System ETRS89 ETRF2000/UTM32 N (EPSG:7791) Walls, CTR- II edition 3D Scale 1:5000 years 2013 Reference System ETRS89 ETRF2000/UTM32 N (EPSG:7791)	A map was produced containing all residential and non-residential buildings, construction structures, as well as retaining structures such as retaining walls and earth retention works. These elements were extracted from the regional topographic database and aggregated into a single layer. To define the area potentially influenced by the presence of these structures on slope behavior, a 10-meter buffer was applied around the selected features.				

Table 11. Description of the map of man-made structures

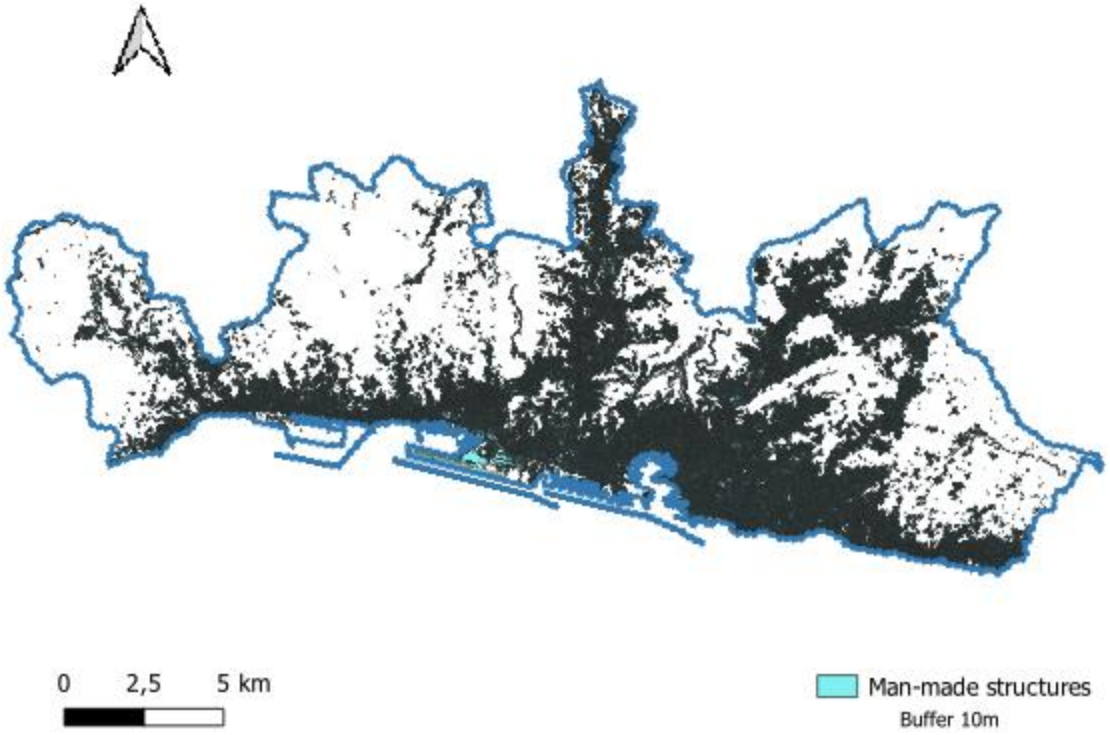

Figure 25. Man-made structures

4.4.12 Past landslides (from the IFFI catalogue)

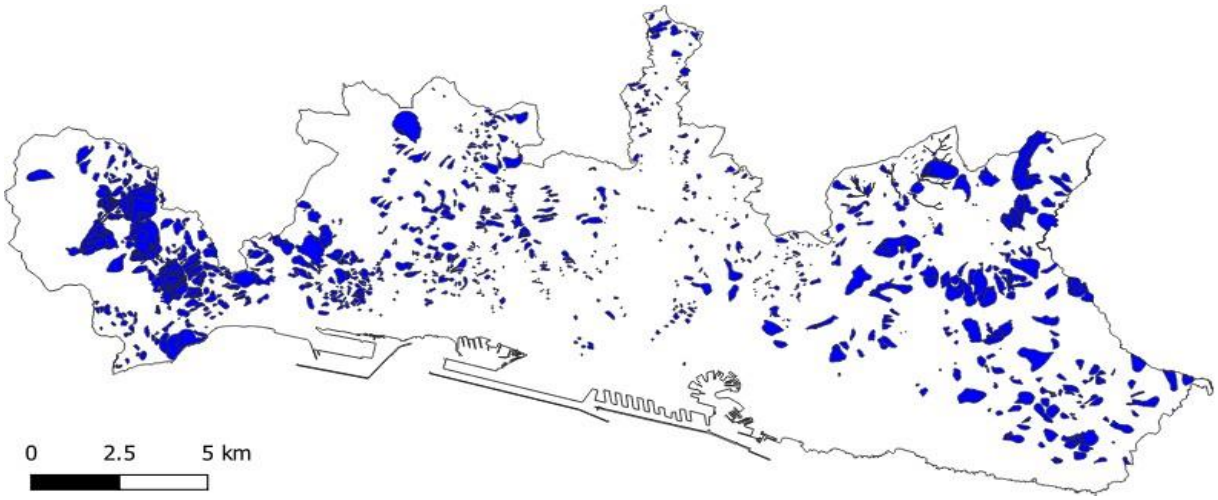

Figure 2c. Existing landslides

In the process of analysing the susceptibility of slopes to surface instability, the presence of pre-existing landslides was also taken into account, as such areas may represent zones characterised by geological, geomorphological and hydrological conditions conducive to the reactivation of mass movements or the triggering of new landslides. Knowledge of historical landslides, in fact, constitutes a significant indicator of the territory's intrinsic predisposition to instability (ISPRA, n.d.).

The data used are taken from the Regional Landslide Catalogue, available at a scale of 1:10,000, in which landslide events are georeferenced, mapped and classified according to the type of

movement (sliding, flow, overturning, etc.) and their state of activity, in accordance with the technical nomenclature commonly adopted in the field of geomorphology.

Landslide phenomena are represented by polygonal geometries that delimit the area affected by the gravitational movement and are accompanied by various descriptive attributes, including the type of movement, the state of activity and further information useful for characterising the phenomenon.

Specifically, for the purposes of the analysis, the following landslide classes were considered, each associated with a different degree of activity and therefore a different level of potential risk:

CLASSIFICATION	MOVEMENT CATEGORY
LANDSLIDE 0	Undetermined landslides
LANDSLIDE 2	Rotational translational slides
LANDSLIDE 4	Slow flows
LANDSLIDE 5	Rapid flows
LANDSLIDE 7	Complex landslides
LANDSLIDE 11	Areas prone to widespread surface landslides

Table 12. IFFI classification (source: https://www.isprambiente.gov.it/it/progetti/cartella-progetti-in-corso/suolo-e-territorio-1/iffi-inventario-dei-fenomeni-franosi-in-italia)

4.5 TESTS CARRIED OUT

This sequence of steps constitutes the methodological framework adopted for the creation of the landslide susceptibility map and forms the analytical basis for the analyses presented in the following sections.

To verify the reliability, limitations and optimal scope of application of the methodology described above, various tests were carried out in the municipality of Genoa.

TEST	DESCRIPTION	DATA	MASK
Study 1.1	Assessment of susceptibility in three classes, taking into account the ARPAL data	ARPAL	Municipality of Genoa
Study 1.2	Assessment of susceptibility in three classes, considering the municipality of Genoa without the influence of the urban area. Climate-related aggressiveness is not taken into account SALSA.1	SALSA.1	Municipality of Genoa excluding the urban area
Study 1.3	Assessment of susceptibility in three classes, also taking into account climatic aggressiveness in 5 classes	SALSA.1	Municipality of Genoa
Study 1.4	Assessment of susceptibility in three classes, taking into account climatic aggressiveness in 6 classes	SALSA.1	Municipality of Genoa
Study 1.5	Assessment of susceptibility taking into account climatic in 6 classes	SALSA.1	Municipality of Genoa excluding the urban area
Study 1.6	Assessment of susceptibility, taking into account climatic aggressiveness in 6 classes and 5 classes of susceptibility	SALSA.1	Municipality of Genoa excluding the urban area
Study 2.1	Assessment of susceptibility considering climatic aggressiveness in 6 classes and 5 classes of susceptibility, repeating the process 10 times	SALSA.1	Municipality of Genoa without urban area
Study 2.2	Assessment of susceptibility considering climatic aggressiveness in 6 classes and 5 susceptibility classes, repeated 10 times	SALSA.1	Metropolitan City of Genoa
Study 2.3	Assessment of susceptibility considering climatic aggressiveness in 6 classes and 5 susceptibility classes, repeating the process 10 times and changing the mask	SALSA.1	Metropolitan City of Genoa and Municipality of Genoa (excluding the urban area)
Study 2.4	Assessment of susceptibility considering climatic aggressiveness in 6 classes and 5 classes of susceptibility, repeating the process 10 times and changing the mask	SALSA.1	Municipality of Genoa and Municipality of Genoa excluding the urban area
Study 2.5	Assessment of susceptibility considering 5 susceptibility classes, repeating it 10 times	ARPAL	Municipality of Genoa

Table 13. Summary description of the studies carried out

4.6 PHASE 1

This phase consisted of individual tests carried out by varying the set of predisposing factors and the study area. It was conducted somewhat randomly, to assess whether it made sense to apply a statistical methodology to the municipality of Genoa and to establish a baseline for both testing the methodology and improving the SALSA.1 procedure.

First, the two sets of predisposing factors, ARPAL and SALSA.1, are considered. Subsequently, climatic aggressiveness is introduced, a factor describing the distribution of precipitation over time. The resulting susceptibility maps are divided into three and five semi-quantitative classes. Finally, to determine the optimal extent for this type of analysis—in order to assess the influence of built-up areas and, more generally, of impervious or heavily modified areas—tests are carried out over different extents.

The most significant tests are described below.

Study 1.1: ARPAL factors covering the municipality of Genoa

- ✓ 70% calibration – 30% validation on complete landslides,
- ✓ 6 types of landslides,
- ✓ landslides n/a excluded due to too few elements,
- ✓ final susceptibility map reclassified into 3 quality classes

Factors considered (ARPAL set):

1. lithology;
2. slope aspect;
3. slope gradient;
4. land use;
5. presence of terraces;
6. hydrographic features (distance from them);
7. roads and distance from them;
8. human-made structures and distance from them;
9. previous landslides derived from the Inventory of Landslide Phenomena in Italy (IFFI)

This analysis yields the following results

Class	1	2	3
Landslide 2	20.29	37.94	41.77
Landslide 4	3.78	45.94	50.28
Landslide 5	13.58	37.99	48.43
Landslide 7	49.06	21.31	29.63
Landslide 11	20.01	38.70	41.29

Table 14. Analysis results for the Genoa area

Class	AUC
Landslide 2	0.7731
Landslide 4	0.945
Landslide 5	0.8504
Landslide 7	0.7447
Landslide 11	0.852

Table 15. AUC analysis results for the Genoa area

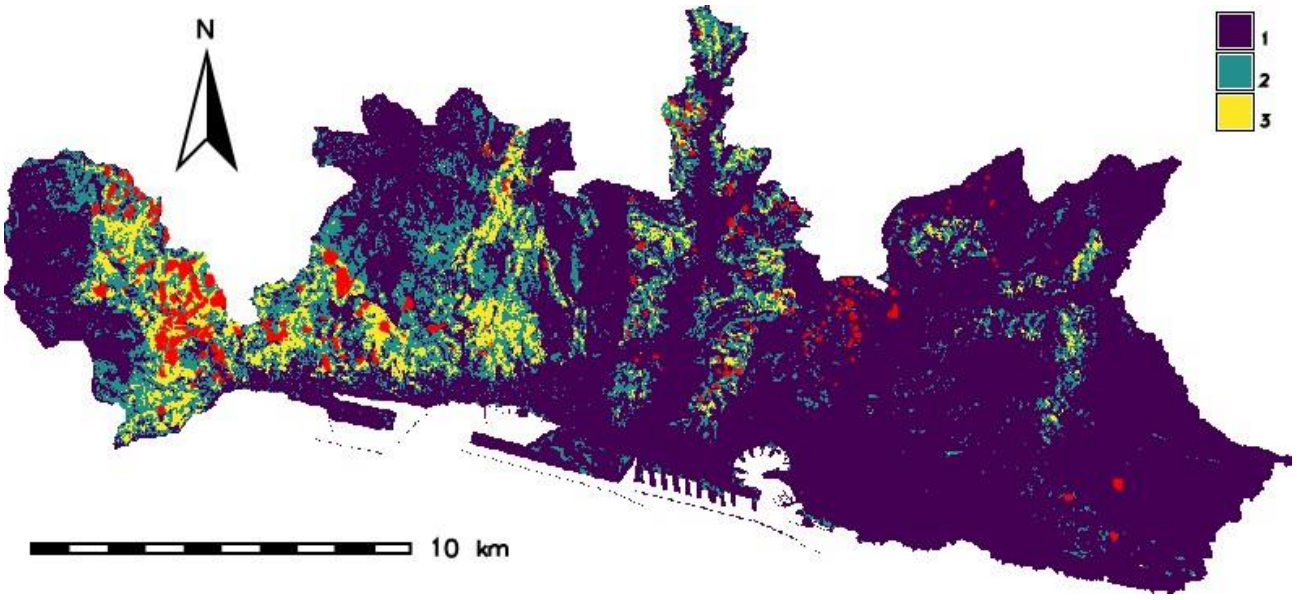

Figure 27: Landslide susceptibility map for areas subject to widespread surface landslides; landslides recorded in the IFFI database are shown in red. The map refers to Study 1

Study 1.2: Municipality of Genoa excluding the built-up area

- ✓ 70% calibration – 30% validation on all landslides,
- ✓ 6 types of landslides,
- ✓ landslides n.a. excluded due to insufficient data,
- ✓ final susceptibility map reclassified into 3 quality classes

In this study, the urban area of the Municipality of Genoa was excluded, as it is characterised by a predominantly rigid surface cover (dense urban fabric, infrastructure, impervious surfaces) and is therefore susceptible to landslide phenomena in a different way compared to areas with natural or semi-natural soil.

To define the new template, the 2018 land use map downloaded from the Liguria Region's Geoportal was used; the following layers associated with the "DESCR_COD_" column were removed from this map:

- airports
- industrial or craft areas
- areas occupied by large public, military and private service facilities (hospitals, etc.)
- commercial and military port areas and those used for fishing
- port areas used mainly for recreational boating
- sports areas
- campsites and tourist accommodation facilities
- sea
- beaches, sand, dunes
- discontinuous and moderately dense residential areas
- discontinuous and scattered residential areas (scattered houses)
- a continuous and dense residential urban fabric
- continuous, moderately dense residential urban fabric

In addition to the automated removal of the identified layers, small residual portions were also manually removed in order to correct cartographic imperfections and ensure greater homogeneity of the final mask.

This methodological choice was made in order to:

- focus the analysis exclusively on areas actually subject to slope instability;
- reduce noise associated with the presence of impermeable or artificial surfaces that are not representative of the phenomena under study;
- improve the statistical reliability of the results obtained by eliminating areas characterised by significantly different geomorphological dynamics;
- increase consistency between observed data and the territorial context.

Considering the SALSA.1 data, the following results are obtained:

Class	1	2	3
Landslide 2	21.64	38.03	40.33
Landslide 4	3.08	48.74	48.18
Landslide 5	24.25	33.37	42.38
Landslide 7	71.21	10.81	17.98
Landslide 11	24.03	32.22	43.75

Table 1c. Results of the analysis for the territory of Genoa excluding the urban area

Class	AUC
Landslide 2	0.7449
Landslide 4	0.9196
Landslide 5	0.7877
Landslide 7	0.6909
Landslide 11	0.8384

Table 17. AUC results for the territory of Genoa excluding the urban area

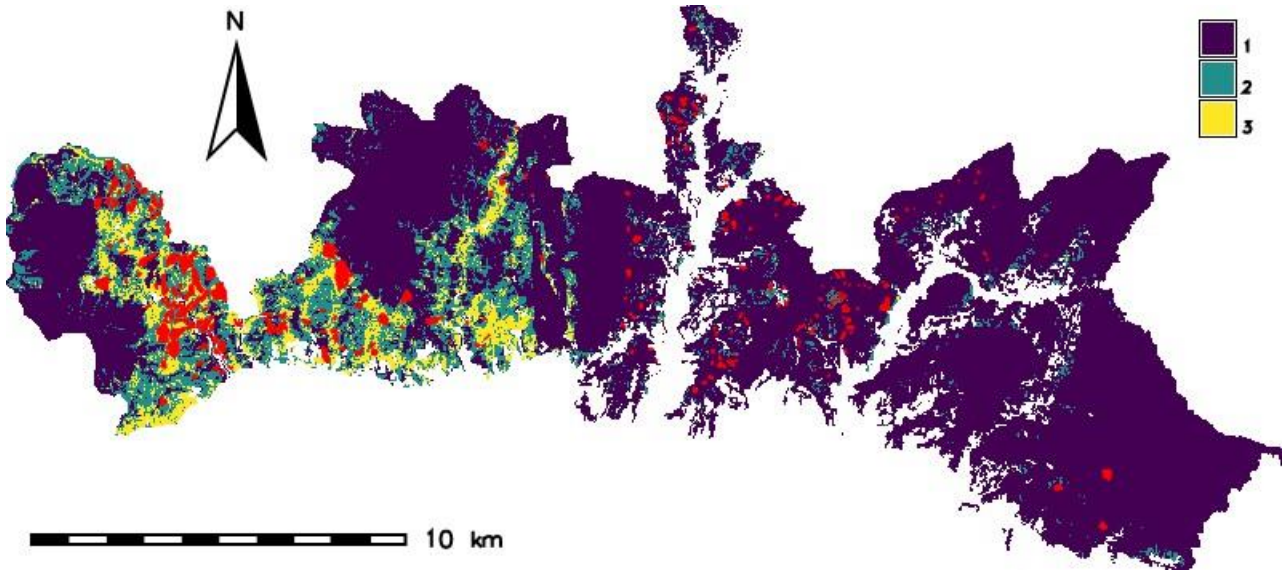

Figure 28. Landslide susceptibility map for areas prone to widespread surface landslides; landslides recorded in the IFFI database are shown in red. The map refers to Study 2

Study 1.3: inclusion of the climatic aggressiveness factor

- ✓ 70% calibration – 30% validation on entire landslides,
- ✓ 6 types of landslides,
- ✓ landslides n/a excluded due to too few elements,
- ✓ final susceptibility map reclassified into 3 qualitative classes
- ✓ climatic aggressiveness is considered in 5 qualitative classes

The stability of a slope depends on the balance between resisting forces and destabilising forces and can be significantly altered by climatic conditions. In particular, intense or prolonged rainfall promotes water infiltration into the ground, leading to an increase in pore pressure and a consequent reduction in effective stress. Since the shear strength of soils is a function of effective stress, an increase in water content results in a decrease in mechanical strength and, therefore, a potential trigger for instability phenomena.

Climate severity is a factor that combines the intensity, duration, frequency and seasonal distribution of meteorological events. It highlights the effect of short, high-intensity rainfall, capable of generating surface runoff and rapid saturation of the surface layers, as well as persistent rainfall events, which promote progressive saturation at depth (Guzzetti et al., 2007). For example, in areas characterised by clayey soils and steep slopes, prolonged autumn rainfall can lead to widespread instability. Similarly, in coastal areas, high-intensity rainfall events concentrated over a few hours can trigger rapid flows and surface landslides on slopes already prone to such events (Guzzetti et al., 2007).

From a hydrogeological perspective, the effect of climate change manifests itself through alterations in the regime of groundwater and surface water. The rise in the water table, the

The formation of suspended layers and the concentration of flow along surfaces of structural discontinuity can promote the development of slip surfaces. Furthermore, in low-permeability cohesive soils, slow but persistent infiltration can induce conditions of neutral overpressure that dissipate over long periods, keeping the slope in a state of precarious equilibrium even after the cessation of the rainfall event (Fredlund C Rahardjo, 1993).

In the context of climate change, the observed increase in the frequency and intensity of extreme weather events makes the integration of climate severity into landslide susceptibility assessment models even more important. The joint analysis of climatic parameters and geological–geomorphological characteristics allows, in fact, for the improved definition of critical rainfall thresholds, spatial planning, and the implementation of risk mitigation and management strategies.

In order to produce the climate severity map and incorporate it as a predisposing factor in the analysis of susceptibility to landslides within the municipality of Genoa, data were collected from weather stations located in the Metropolitan City of Genoa, including station names, geographical

coordinates (latitude and longitude), and monthly and annual cumulative precipitation values. This information was organised into an Excel database, prepared for subsequent processing in a GIS environment. The data was obtained from the official website of the Liguria Region.

Using QGIS software, each weather station was georeferenced based on the available coordinates, creating a point layer accompanied by an attribute table containing monthly precipitation values.

Once the data layer had been created, the rainfall data was spatially interpolated. Specifically, for each column of the attribute table corresponding to the monthly total, the IDW[2] (Inverse Distance Weighting) interpolation method was applied, generating a total of 264 raster maps covering the province. Each raster represents the spatial distribution of average monthly precipitation over the reference period considered (2002–2024).

Subsequently, the rasters obtained were organised into separate directories for each year of analysis, containing the relevant monthly averages, and imported into the GRASS GIS environment for further processing. Within the GRASS environment, using the r.mapcalc command, the following steps were carried out:

- calculation of the average precipitation for each month over the entire reference period (23 years);

$$\sum_{i=anno} precipitazione\ media\ mensile(i) / n\ anni$$

Example for the month of January (this step must be repeated for all months)

$$media\_gen\_02\_24@medie$$
$$= (gen\_2002@A\_2002 + gen\_2003@A\_2003 + gen\_2004@A\_2004$$
$$+ gen\_2005@A\_2005 + gen\_2006@A\_2006 + gen\_2007@A\_2007$$
$$+ gen\_2008@A\_2008 + gen\_2009@A\_2009 + gen\_2010@A\_2010$$
$$+ gen\_2011@A\_2011 + gen\_2012@A\_2012 + gen\_2013@A\_2013$$
$$+ gen\_2014@A\_2014 + gen\_2015@A\_2015 + gen\_2016@A\_2016$$
$$+ gen\_2017@A\_2017 + gen\_2018@A\_2018 + gen\_2019@A\_2019$$
$$+ gen\_2020@A\_2020 + gen\_2021@A\_2021 + gen\_2022@A\_2022$$
$$+ gen\_2023@A\_2023 + gen\_2024@A\_2024) / 23$$

- calculation of average annual precipitation

$$\sum_{i=mese} precipitazione\ media\ mensile(i) / 12$$

Example for the year 2002 (to be repeated for each year):

$$tot\_2002@A\_2002$$
$$= (gen\_2002@A\_2002 + feb\_2002@A\_2002 + marz\_2002@A\_2002$$

[2] Inverse Distance Weighting (IDW) interpolation estimates unknown values by specifying the search distance, nearest points, and power setting C barriers

+ ap_2002@A_2002 + mag_2002@A_2002 + giu_2002@A_2002
+ lug_2002@A_2002 + ag_2002@A_2002 + $sett$_2002@A_2002
+ ott_2002@A_2002 + nov_2002@A_2002 + gen_2002@A_2002/ 12

- calculation of the average annual precipitation over the same time period

$$\sum_{i=anno} precipitazione\ media\ annua(i) / n\ anni$$

Example:

(tot_2002@A_2002 + tot_2003@A_2003 + tot_2004@A_2004 + tot_2005@A_2005
+ tot_2006@A_2006 + tot_2007@A_2007 + tot_2008@A_2008
+ tot_2009@A_2009 + tot_2010@A_2010 + tot_2011@A_2011
+ tot_2012@A_2012 + tot_2013@A_2013 + tot_2014@A_2014
+ tot_2015@A_2015 + tot_2016@A_2016 + tot_2017@A_2017
+ tot_2018@A_2018 + tot_2019@A_2019 + tot_2020@A_2020
+ tot_2021@A_2021 + tot_2022@A_2022 + tot_2023@A_2023
+ tot_2024@A_2024) / 23

- calculation of the climate aggressiveness index based on monthly and annual average values.

$$\sum \exp\left(\frac{\text{precipitazione media di ciascun mese sull'intero periodo di riferimento}}{\text{precipitazione media annua}}\right.$$

Esempio

$(exp(\ media\_gen\_02\_24@medie\ ,2)/\ media\_annua\_02\_24@medie\ )$
$+\ (exp(\ media\_feb\_02\_24@medie\ ,2)/\ media\_annua\_02\_24@medie\ )$
$+\ (exp(\ media\_mar\_02\_24@medie\ ,2)/\ media\_annua\_02\_24@medie\ )$
$+\ (exp(\ media\_apr\_02\_24@medie\ ,2)/\ media\_annua\_02\_24@medie\ )$
$+ (exp(\ media\_mag\_02\_24@medie\ ,2)/\ media\_annua\_02\_24@medie\ )$
$+\ (exp(\ media\_giu\_02\_24@medie\ ,2)/\ media\_annua\_02\_24@medie\ )$
$+\ (exp(\ media\_lug\_02\_24@medie\ ,2)/\ media\_annua\_02\_24@medie\ )$
$+\ (exp(\ media\_ago\_02\_24@medie\ ,2)/\ media\_annua\_02\_24@medie\ )$
$+\ (exp(\ media\_set\_02\_24@medie\ ,2)/\ media\_annua\_02\_24@medie\ )$
$+\ (exp(\ media\_ott\_02\_24@medie\ ,2)/\ media\_annua\_02\_24@medie\ )$
$+\ (exp(\ media\_nov\_02\_24@medie\ ,2)/\ media\_annua\_02\_24@medie\ )$
$+\ (exp(\ media\_dic\_02\_24@medie\ ,2)/\ media\_annua\_02\_24@medie\ )$

This procedure was used to produce the map of average climatic aggressiveness (Figure 23) for the period 2002–2024, derived from the analysis of average monthly and annual precipitation values. The final product is a continuous raster layer, representing the spatial distribution of the average intensity of the climatic factor, subsequently used as a predisposing factor in the landslide susceptibility model.

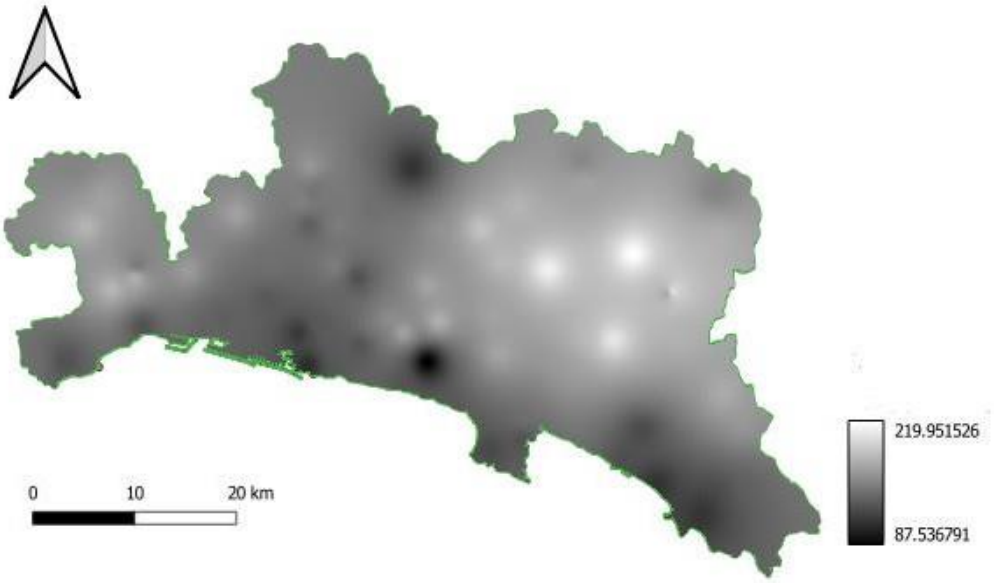

Figure 2S. Climate aggressiveness in the Metropolitan City of Genoa

To analyse the influence of this new predisposing factor, the CORINE-CEC classification was used in an initial phase (Table 18).

Class	*Range*
High class	> 160
Upper-middle class	160–120
Middle class	120–90
Lower-middle class	90–60
Lower class	< 60

Table 18: Classification of climatic aggressiveness used by CORINE-CEC, 1SS2. CORINE soil erosion risk and important land resources. An assessment to evaluate and map the distribution of land quality and soil erosion risk. Office for Official Publications of the European Communities. EUR 13233. Luxembourg.

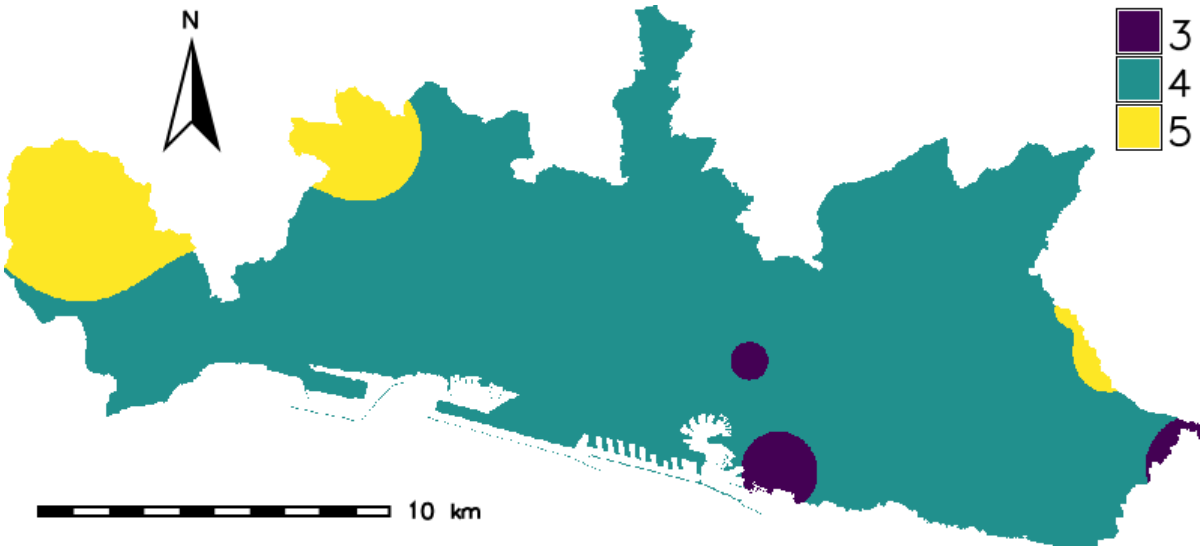

Figure 30. Climate aggressiveness map of the Genoa area in 5 classes

For the area under consideration, the low and lower-medium classes are not represented; therefore, in practice, only three classes are present. The study was carried out within the municipality of Genoa (Study 3), yielding the following result:

Class	*1*	*2*	*3*
Landslide 2	13.04	40.48	46.46
Landslide 5	7.26	45.84	46.90
Landslide 7	34.67	30.05	35.28
Landslide 11	16.93	37.94	45.13

Table 1S. Results of the analysis for the Genoa area

Class	*AUC*
Landslide 2	0.7819
Landslide 5	0.818
Landslide 7	0.7411
Landslide 11	0.8438

Table 20. AUC results for the Genoa area

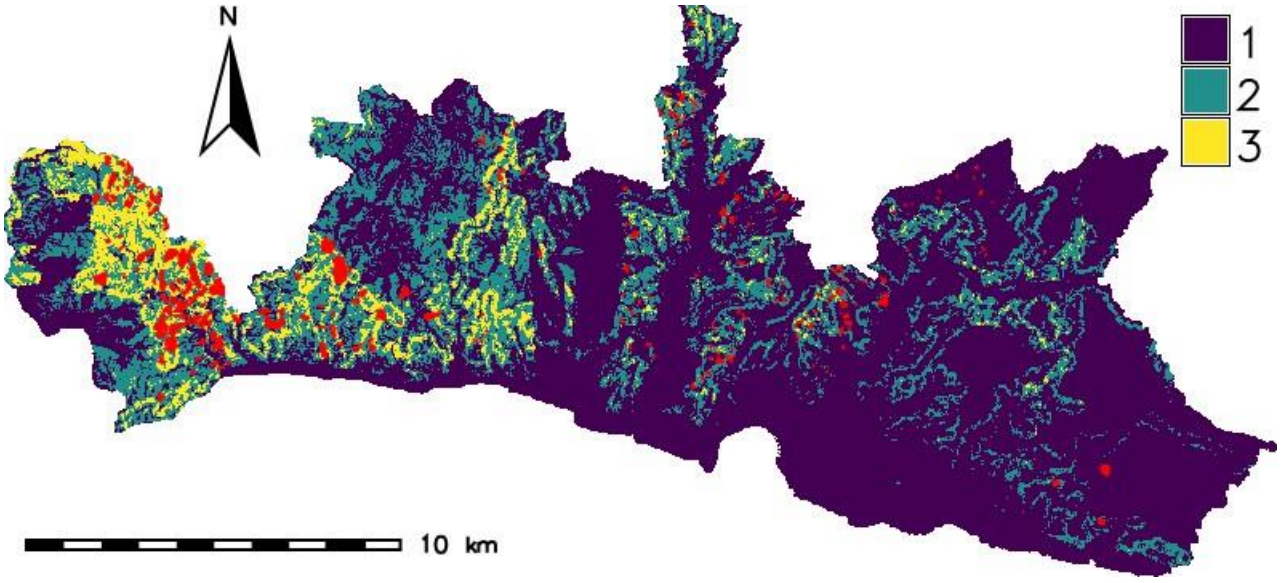

Figure 31. Landslide susceptibility map for areas subject to widespread surface landslides; landslides recorded in the IFFI database are shown in red. The data refer to Study 3

Studies 1.4 and 1.5: use of 6 classes of climatic aggressiveness

- ✓ 70% calibration – 30% validation on entire landslides,
- ✓ 6 types of landslides,
- ✓ landslides (n/a) excluded due to insufficient data,
- ✓ final susceptibility map reclassified into 3 qualitative classes,
- ✓ climatic aggressiveness is considered in 6 qualitative classes

To achieve greater detail and a more detailed description of the spatial variability of climatic aggressiveness, the factor was reclassified into six classes.

This allowed the classification of climatic aggressiveness to be adapted to the specific context of the study, reducing any oversimplifications resulting from an overly general subdivision and improving the model's ability to highlight differences between areas. This made it possible to assess more effectively the influence of precipitation on the terrain's susceptibility to slope instability.

The climatic aggressiveness classes adopted in the study are shown in the table below.

Class	*Range*
Very high class	> 160
High class	160–140
Upper-middle class	140–120
Middle class	120–90
Lower-middle class	90–60
Lower class	< 60

Table 21. New classification of climatic aggressiveness

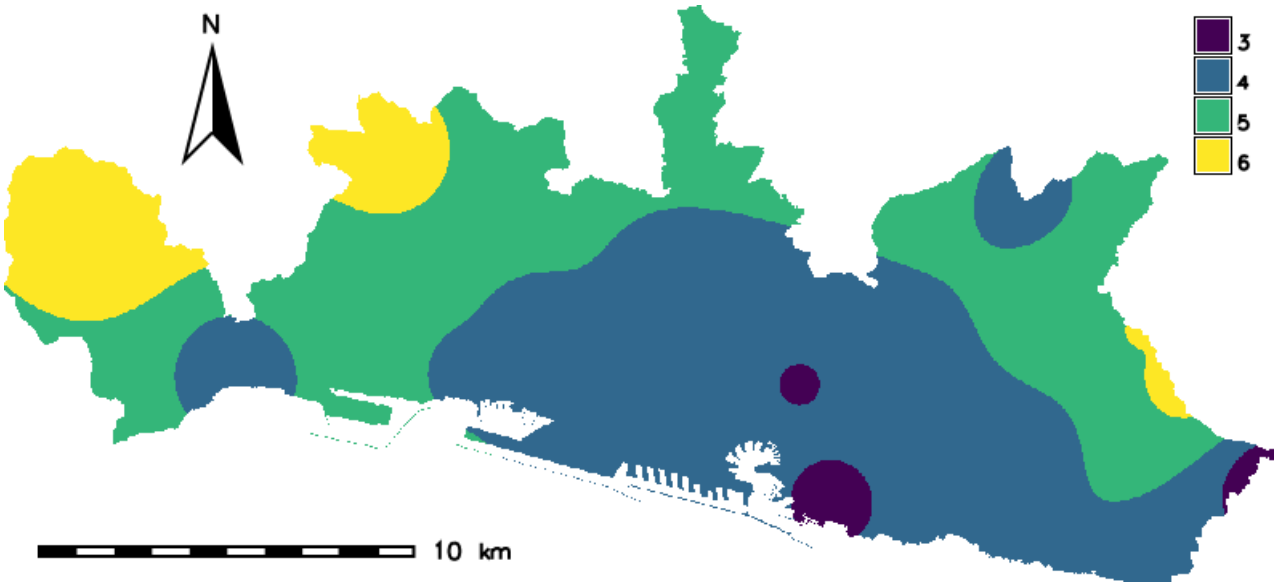

Figure 32. Map of climatic aggressiveness in the municipality of Genoa, classified into three classes

Using the municipality of Genoa as a mask (Study 4), the following data are obtained

Class	*1*	*2*	*3*
Landslide 2	14.98	41.57	43.44
Landslide 4	4.51	44.21	51.28
Landslide 5	8.77	40.79	50.44
Landslide 7	36.31	29.97	33.72
Landslide 11	13.9	39.24	46.86

Table 22. Results of the analysis for the Genoa area

Class	*AUC*
Landslide 2	0.7819
Landslide 4	0.9257
Landslide 5	0.8435
Landslide 7	0.749
Landslide 11	0.8443

Table 23. AUC results for the Genoa area

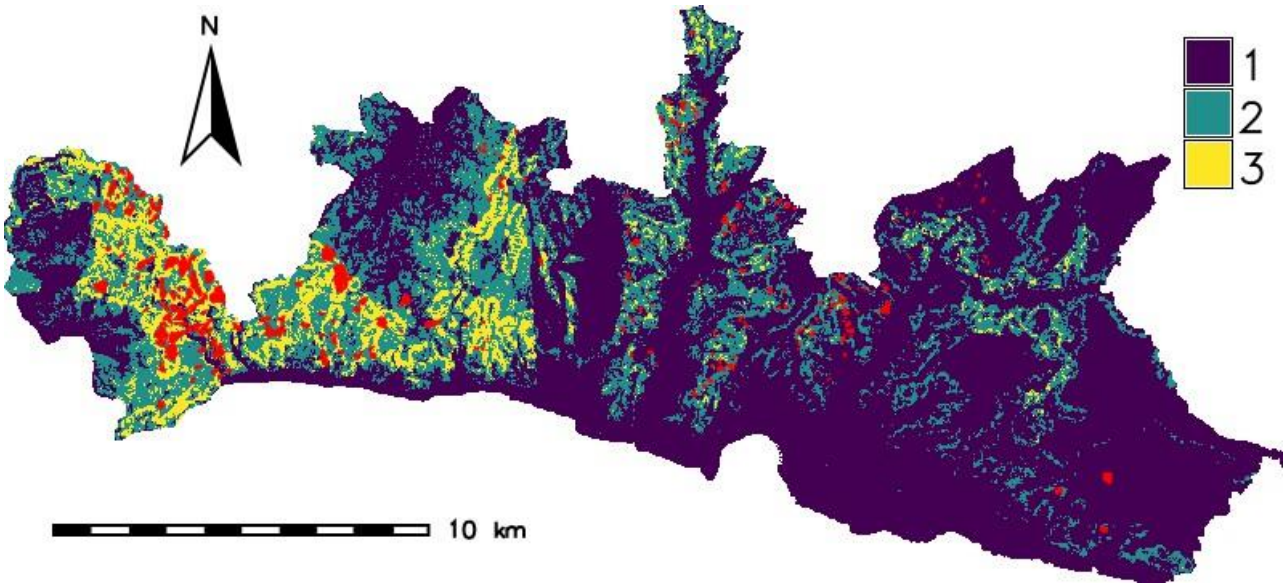

Figure 33. Landslide susceptibility map for areas subject to widespread surface landslides; landslides recorded in the IFFI database are shown in red. The map refers to Study 4

Using instead the municipality of Genoa without the built-up area as a mask (Study 5) yields the following results

Class	*1*	*2*	*3*
Landslide 2	14.68	41.77	43.55
Landslide 4	9.63	41.53	48.84
Landslide 5	19.35	37.95	42.71
Landslide 7	56.83	19.28	23.89
Landslide 11	21.37	31.69	46.94

Table 24. Results of the analysis for the municipality of Geova, excluding the urban area

Class	*AUC*
Landslide 2	0.7366
Landslide 4	0.9255
Landslide 5	0.8054
Landslide 7	0.6907
Landslide 11	0.8367

Table 25. AUC results for the municipality of Genoa excluding the urban area

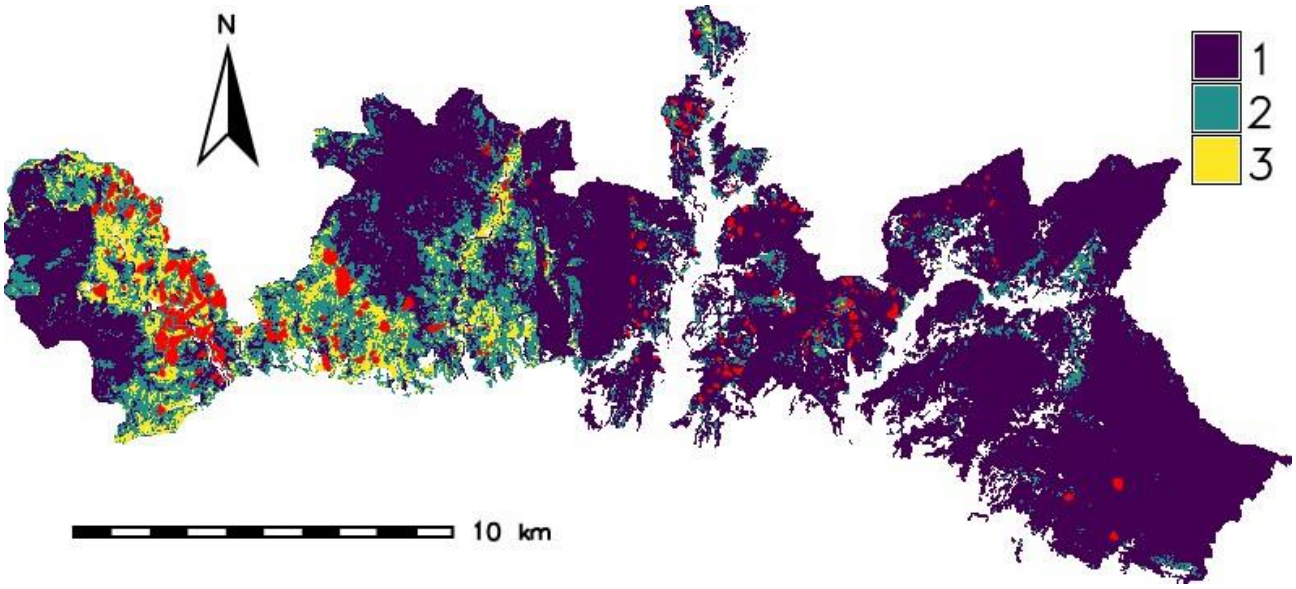

Figure 34. Landslide susceptibility map for areas prone to widespread surface landslides; landslides recorded in the IFFI database are shown in red. The map refers to Study 5

Study 1.6: use of 5 susceptibility classes

- ✓ 70% calibration – 30% validation on all landslides,
- ✓ 6 types of landslides,
- ✓ landslides (n/a) excluded due to insufficient data,
- ✓ final susceptibility map reclassified into 5 qualitative classes,
- ✓ climatic aggressiveness is considered in 6 qualitative classes

A further case study considered in the analysis involves the use of a susceptibility classification divided into five classes. The division into five classes allows for a more accurate distinction between areas characterised by very low, low, moderate, high and very high susceptibility, improving the spatial interpretation of the results and providing more effective support for subsequent stages of analysis and assessment.

The class intervals were defined on the basis of the landslide area values. Specifically, the first class comprises the interval between 0 and the minimum value of the landslide area observed in the dataset. The fifth class, on the other hand, includes values above the average landslide area. The three intermediate classes were determined by dividing the range between the minimum value and the average landslide area into three intervals of equal width.

Taking this classification into account and using the municipality of Genoa (excluding the urban centre) as a mask, the following results are obtained

Class	1	2	3	4	5
Landslide 2	0	7.14	24.14	24.58	44.14
Landslide 4	0.06	3.7	10.78	27.91	57.55
Landslide 5	0.01	1.86	14.52	36.26	47.35
Landslide 7	0	44.87	23.06	10.52	21.54
Landslide 11	0	13.91	15.15	21.42	49.52

Table 2c. Results of the analysis in the municipality of Genoa excluding the urban centre

Class	AUC
Landslide 2	0.743
Landslide 4	0.9134
Landslide 5	0.8187
Landslide 7	0.6913
Landslide 11	0.836

Table 27. AUC results for the municipality of Genoa excluding the urban centre

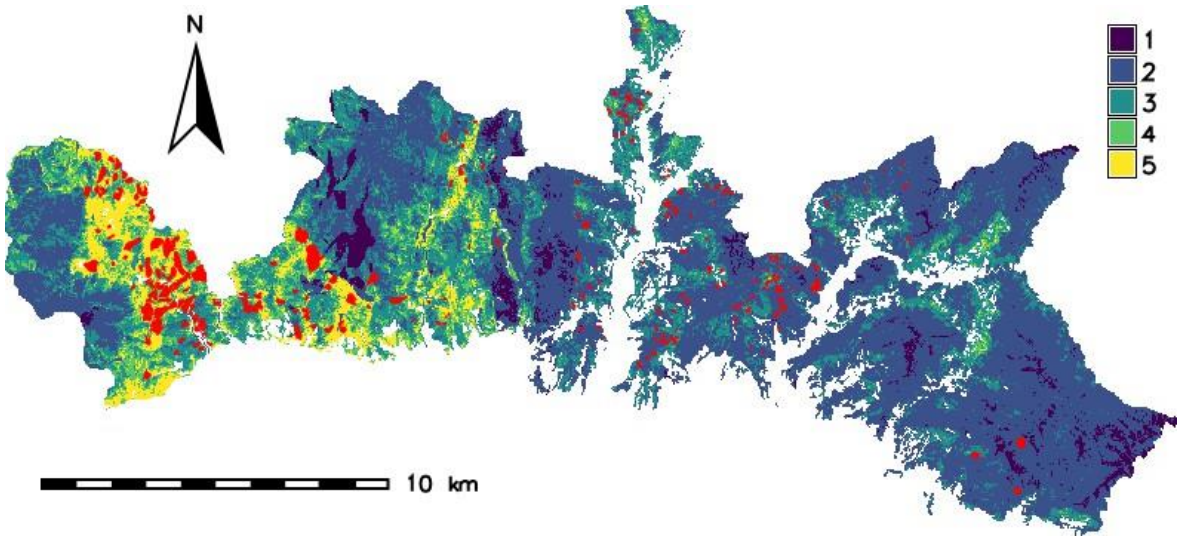

Figure 35. Landslide susceptibility map for areas subject to widespread surface landslides; landslides recorded in the IFFI database are shown in red. The map refers to study c

4.6.1 Phase 1 considerations

During the first stage of processing, a critical issue arose concerning the script “fr_0999_01_tipi_di_frana_franaW”, which also included landslide class 0, despite this being represented by a single data point. The presence of this value caused a malfunction in the subsequent processing stages, specifically blocking the procedure for selecting combinations between the various factors. To resolve the issue, a check was therefore introduced into the script, designed to automatically exclude from the procedure landslide types characterised by a number of polygons below a certain threshold, provisionally set at 10 units.

At the same time, a review was carried out of the variables used as inputs in the model. At this stage, the variable relating to terracing was removed, as it was already indirectly represented within the land-use class, thus avoiding potential problems of collinearity between the factors under consideration. In its place, the climate aggressiveness parameter was introduced, considered one of the most significant elements in assessing susceptibility to landslide phenomena.

A comparative analysis of the various configurations tested showed that the most effective combination is achieved by using the climatic aggressiveness index divided into 6 classes and a susceptibility map divided into 5 classes. This configuration yielded results that were more consistent and better representative of the distribution of landslide phenomena in the study area.

Overall, this initial phase of the analysis proved crucial for verifying the consistency and validity of the methodological approach adopted, as well as enabling an initial selection and definition of the most relevant factors to be included in the model.

At the same time, it allowed for reflection on the most appropriate spatial extent of the study area. In particular, it emerged that urbanised areas exhibit different dynamics compared to natural contexts; however, their a priori exclusion would result in the loss of the influence exerted by the surrounding slopes on water accumulation and conveyance processes, as well as altering the distribution of distance bands from transport routes.

Similarly, the rigid adoption of administrative boundaries as the limit of the analysis area would lead to the exclusion of the influence of immediately external morphological factors, which may instead play a significant role in the processes analysed.

4.7 PHASE 2

After resolving the main issues that emerged in the first phase of processing, an additional script, named GE_fr_09_cambia_maschera, was introduced to reduce the study area following the first phase of bivariate statistics. Subsequently, further case studies were analysed in order to assess the influence of spatial extent and the selection of the territorial mask on the model's results.
The following analysis scenarios were therefore considered:

- Case study with a mask corresponding to the Municipality of Genoa, excluding the built-up area, in order to reduce possible interference due to high levels of urbanisation.
- Case study with a mask covering the entire Metropolitan City of Genoa, to assess the model's behaviour on a larger territorial scale.
- Case study with an initial mask covering the Metropolitan City of Genoa, followed by a subsequent change of mask, to analyse the effect of the variation in the reference area during the modelling process.
- Case study with an initial mask covering the Municipality of Genoa, followed by a subsequent change of mask, to compare the results obtained with those of the previous case and verify any differences due to the initial scale of analysis.
- Case study based on data suggested by ARPAL, for an evaluative comparison

For each case study, the entire processing procedure was repeated ten times, with the aim of analysing the variability of the results and assessing the stability of the model. This procedure allowed us to observe the fluctuations in the values obtained and to calculate certain descriptive statistical indicators, including the mean, median and standard deviation, which are useful for a more robust and comparable evaluation of the results. The values of the model's performance indicators, in particular AUC (Area Under the Curve), AIC (Akaike Information Criterion) and the susceptibility percentage, differ even when the same case study is applied. This is due to the fact that, at each run, the software automatically selects different data samples for the model's calibration and validation phase.
This random sampling process introduces inherent variability into the results, making it necessary to perform a statistical analysis of the repetitions to obtain representative values.
During the processing, the following scripts were applied, executed in the following order:

1) GE_fr_01_settings_W
2) GE_fr_02_import_DTM_W
3) GE_fr_03_slope_exposure_acc_W
4) GE_fr_04_elevation_reclass_W

5) GE_fr_05_lithology_W
6) GE_fr_06_transport_W
7) GE_fr_07_land_use_W
8) GE_fr_08_climatic_aggregate_W
9) GE_fr_09_change_layer (to be used only when changing layers)
10) GE_fr_0999_01_types_of_landslide_landslideW
11) GE_fr_0999_02_valid_landslide_calibration_W
12) GE_fr_1000_prob_cond_csv_W
13) GE_fr_1001_reorder_classes_correct
14) GE_fr_1002_reclassify_factors_W
15) GE_fr_1003_logit_W
16) GE_fr_1004_COMBOS_W
17) fr_1005_univariate_susceptibility_W (run twice)
18) fr_1006_5_classes_susceptibility_W
19) fr_1007_report_for_5_classes_W

Study 2.1: using the municipality of Genoa (excluding the urban centre) as a mask

The results of the first study highlight significant differences in the behaviour of the landslides analysed between the model's calibration and validation phases. In particular, landslide 4 shows marked variations in the validation phase, especially in classes 3 and 4 (Figures 35 and 36), indicating greater sensitivity of the model in the higher susceptibility classes. Significant variations in behaviour are also observed for landslide 5.

For landslide 11, however, the variations are generally limited and occur mainly during the calibration phase, suggesting greater stability of the results across the different classes considered.

Landslide 7 generally shows limited variations between classes; however, class 2 exhibits more significant deviations compared to the others, indicating a less homogeneous distribution of values (Figures 37 and 38). Analysis of the average percentages for each landslide shows particularly positive results for landslides 11 and 2 (Figures 39 and 40).

In these cases, in fact, the sum of the percentages associated with the medium-high and high classes exceeds 70%, which is significantly higher than for the low and medium-low classes. This data suggests that the model is capable of correctly identifying areas of higher susceptibility. Conversely, the average values for landslide 7 (Figure 41) show less satisfactory performance, indicating a lower discriminatory capacity of the model in this specific case.

Class	AUC CAL	AUC VAL
Landslide 2	0.7416	0.7186
Landslide 4	0.9249	0.8436
Landslide 5	0.8114	0.7421
Landslide 7	0.6976	0.6651
Landslide 11	0.8324	0.8370

Table 28. AUC results from study 1.1

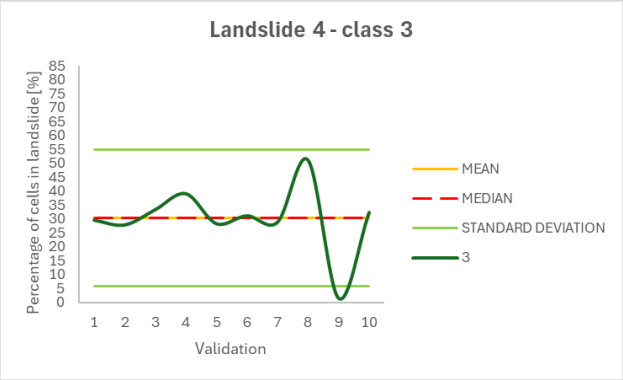

Figure 3c. Mean, median and standard deviation values for landslide 4, class 3 in validation

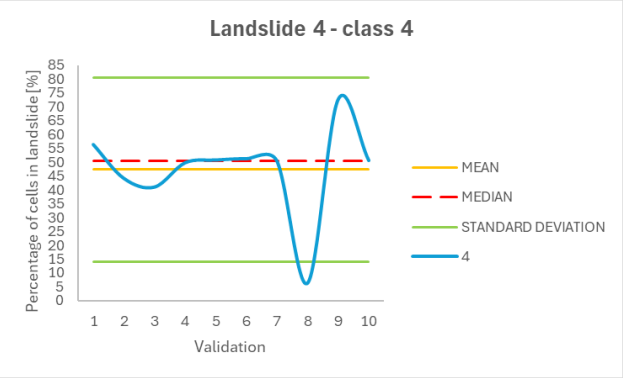

Figure 37. Mean, median and standard deviation values for landslide 4, class 3 in validation

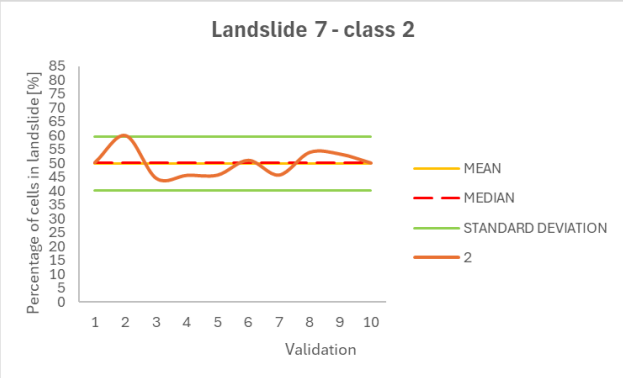

Figure 38 Mean, median and standard deviation values for landslide 7, class 2 in validation

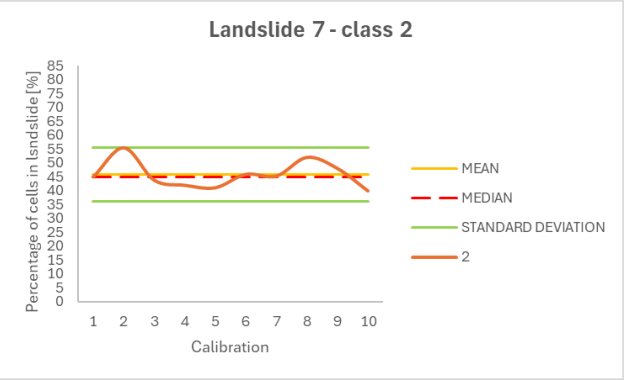

Figure 3S Mean, median and standard deviation values for landslide 7, class 2 in calibrat

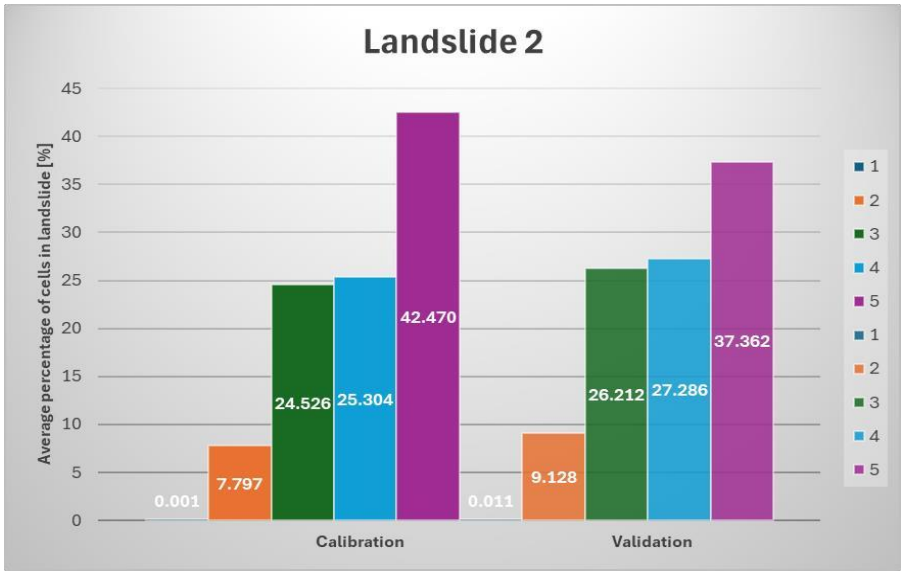

Figure 40. Graph of percentage averages for landslide 2

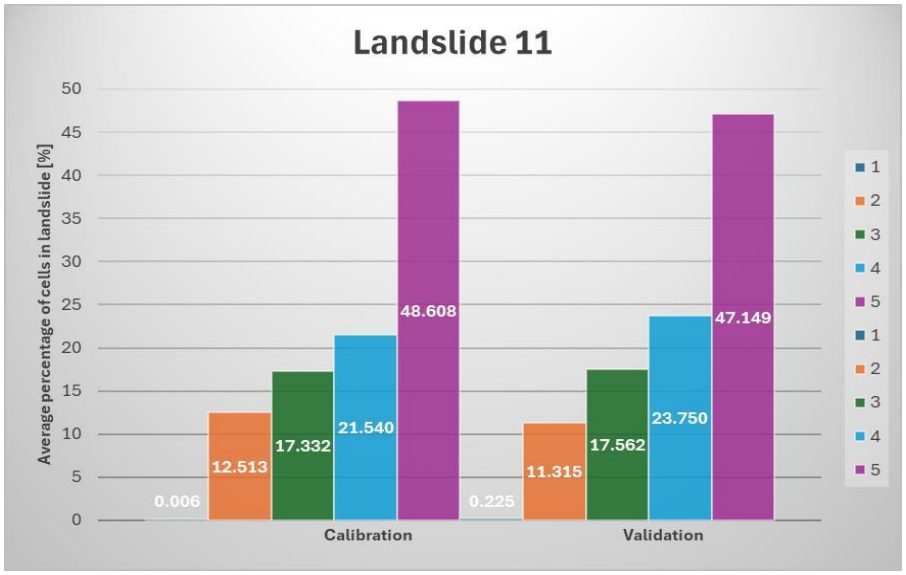

Figure 41. Graph of average percentages for landslide 11

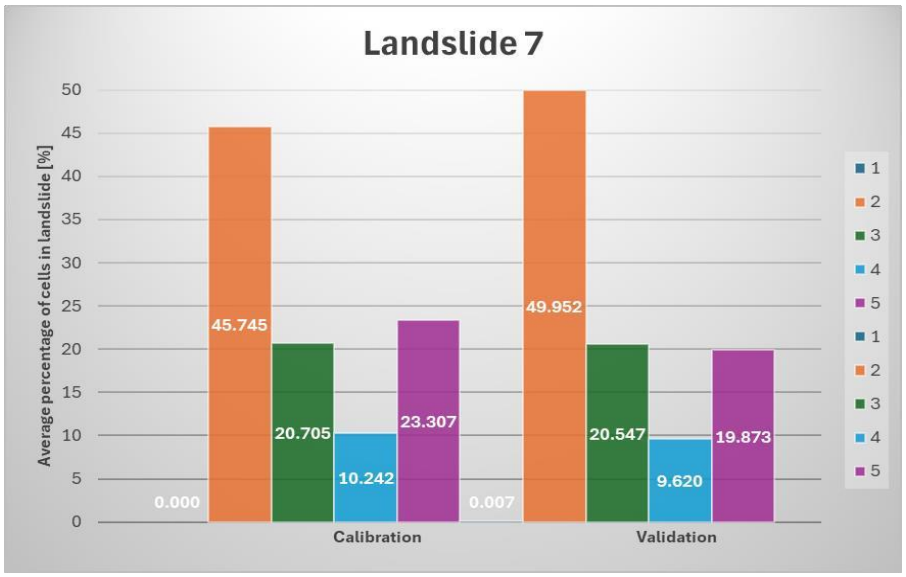

Figure 42. Graph showing the average percentage of landslide 7

Study 2.2 using the Metropolitan City of Genoa as a mask

The results show generally positive performance for landslide 4, with no particularly significant variations in the distribution of values across the different classes.In the case of landslide 5, however, more marked deviations are observed, particularly during the validation phase, where the variations are most evident in classes 3 and 5 (Figures 43 and 44).

Landslide 7 shows limited variations, concentrated mainly in class 2, in both the calibration and validation phases (Figures 45 and 46). For landslide 11, more significant deviations are recorded in class 5 (Figure 47). However, it is important to note that all values fall within the range defined by ±2 standard deviations, indicating that the variability of the results is generally limited. Finally, the analysis of the percentage means reveals less satisfactory results for landslide 7 (Figure 48), suggesting that the model is less capable of correctly representing the class distribution compared to the other cases analysed.

Class	*AUC CAL*	*AUC VAL*
Landslide 2	0.6904	0.6618
Landslide 4	0.7972	0.7782
Landslide 5	0.7842	0.7682
Landslide 7	0.7150	0.6921
Landslide 11	0.7999	0.7952

Table 2S. AUC results from Study 1.2

Figure 43. Mean, median and standard deviation values for landslide 5, class 3 in validation

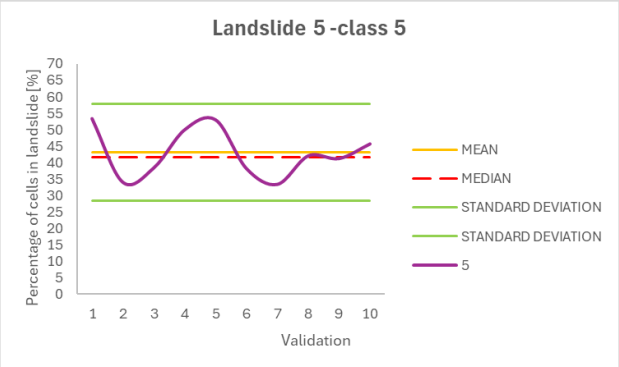

Figure 44. Mean, median and standard deviation values for landslide 5, class 5 in validation

Figura 45 *Mean, median and standard deviation values for landslide 7, class 2 in validation*

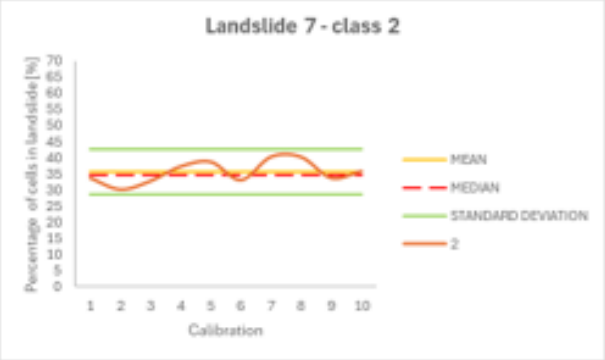

Figura 46. *Mean, median and standard deviation values for landslide 7, class 2 in calibration*

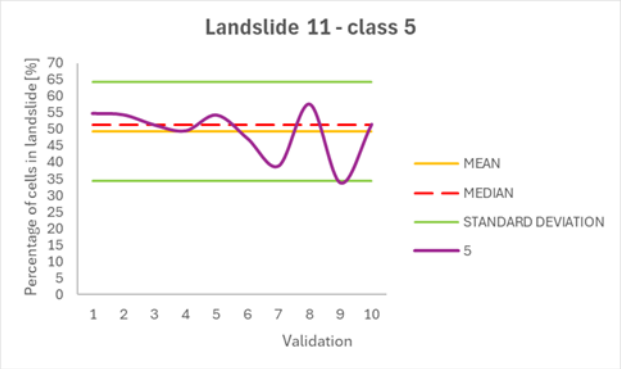

Figure 47. Mean, median and standard deviation values for landslide 11, class 5 in validation

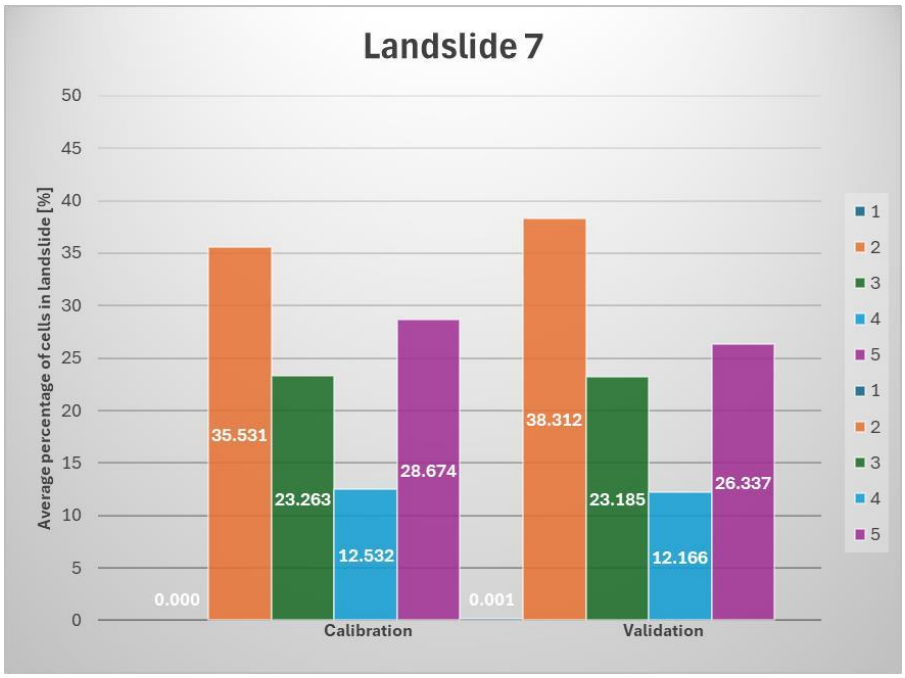

Figure 48. Graph of percentage averages for landslide 7

Study 2.3 using the Metropolitan City of Genoa as a mask, with a subsequent change of mask

Analysis of the results highlights differences in the behaviour of the landslides under consideration between the model's calibration and validation phases. In particular, landslide 5 shows more pronounced variations during the validation phase, especially in classes 2 and 5 (Figures 49 and 50), whereas in the calibration phase the values are generally more stable and characterised by limited variability. In the case of landslide 7, slightly more pronounced deviations are observed in class 2, present in both the calibration and validation phases (Figures 51 and 52), suggesting greater sensitivity of the model in representing this specific class. Landslide 11, on the other hand, shows greater variations significant during the validation phase, particularly in class 5 (Figure 53), whilst no significant differences emerge between the analysed classes during calibration. It is important to note, however, that the set of values always remains within the range defined by ±2 standard deviations, indicating that the dispersion of the results is statistically limited and does not reveal any significant anomalies.

Analysis of the mean values also confirms a less satisfactory performance for landslide 7 (Figure 54) compared to the other cases studied, suggesting a reduced ability of the model to correctly represent the class distribution for this specific event.

Class	*AUC CAL*	*AUC VAL*
Landslide 2	0.7496	0.7052
Landslide 5	0.8201	0.6362
Landslide 7	0.7050	0.6572
Landslide 11	0.8409	0.8072

Table 30. AUC results from study 1.3

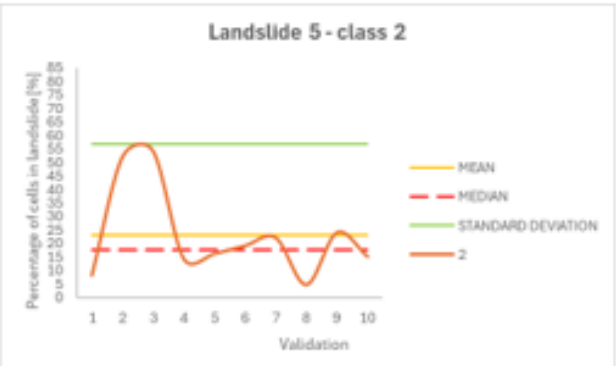

Figura 49. Mean, median and standard deviation values for landslide 5, class 2 in validation

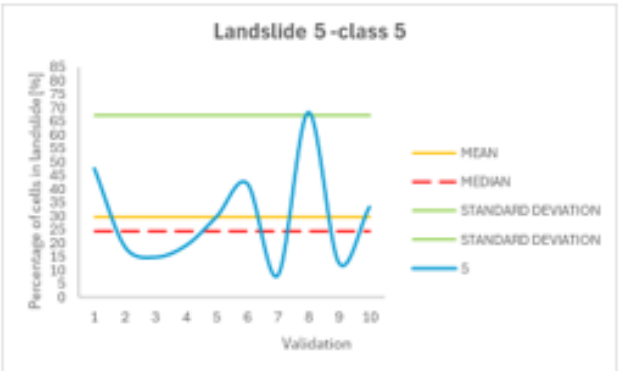

Figura 50. Mean, median and standard deviation values for landslide 5, class 5 in validation

Figura 51. Mean, median and standard deviation values for landslide 7, class 2 in validation

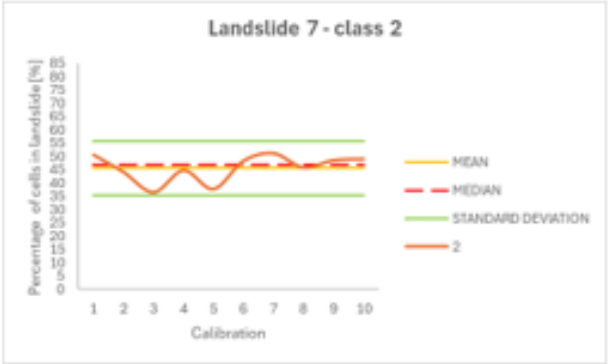

Figura 52. Mean, median and standard deviation values for landslide 7, class 2 in calibration

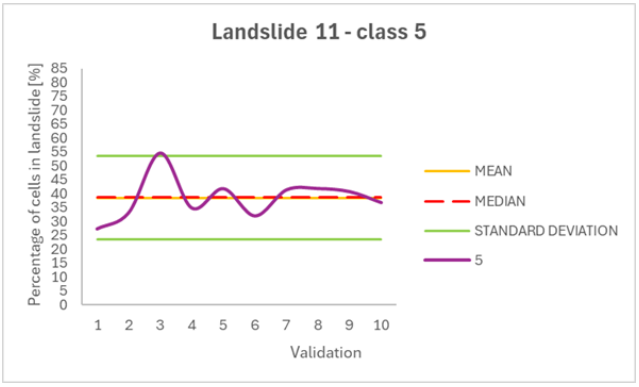

Figure 53. Mean, median and standard deviation values for landslide 11, class 5, under validation

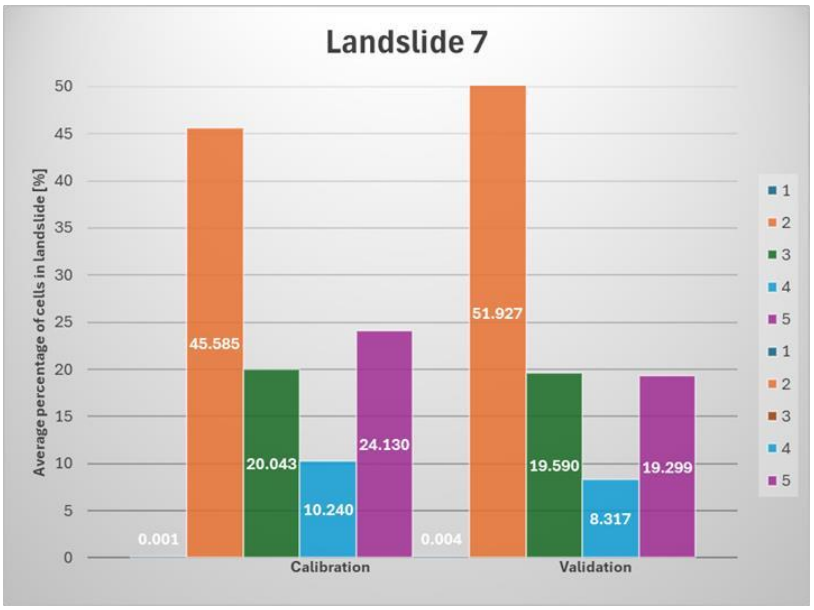

Figure 54. Graph of average percentages for landslide 7

Study 2.4: use of the municipality of Genoa as a mask, followed by a change of mask

Analysis of the results reveals marked variations for landslide 5 (Figure 56) and, to a slightly lesser extent, for landslides 2 and 11 (Figure 55), particularly during the validation phase. A different pattern is observed for landslide 7, for which the variations are concentrated mainly in class 2 and are more evident during the validation phase. Finally, analysis of the mean values reveals less satisfactory performance for landslide 7 (Figure 57).

Class	*AUC CAL*	*AUC VAL*
Landslide 2	0.7465	0.7038
Landslide 5	0.8125	0.6766
Landslide 7	0.7048	0.6645
Landslide 11	0.8396	0.8055

Table 31. AUC results from Study 1.4

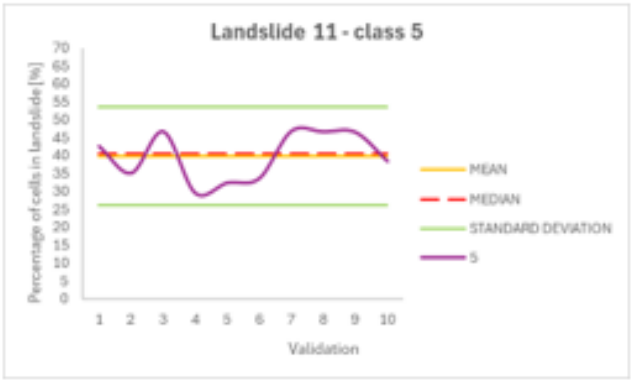

Figure 55. Mean, median and standard deviation values for landslide 11, class 5 in validation

Figure 56. Mean, median and standard deviation values for landslide 5, class 5 in validation

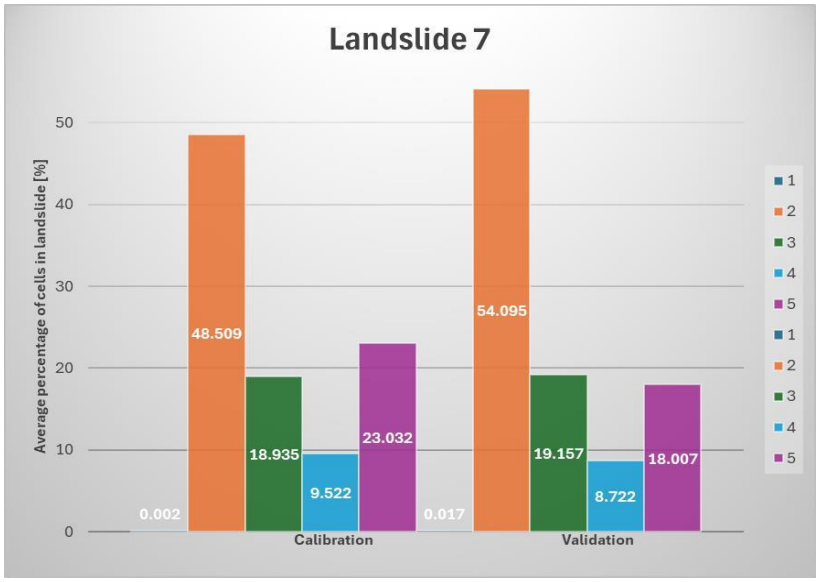

Figure 57. Graph of average percentages for landslide 7

Study 2.5: use of the ARPAL dataset

The integration of the ARPAL data led to an improvement in the mean values, particularly for landslide 7 (Figure 60). The most significant deviations from the other results are concentrated in landslide 7, with marked variations in class 2 (Figure 59), observable in both the calibration and validation phases (Figure 58), and in class 5 during validation. Significant differences also emerge for landslide 5 during the validation phase (see Figure 58) and for landslide 2 in class 5, again during the validation phase. Using the municipality of Genoa as a mask, the following results are obtained:

Class	*AUC CAL*	*AUC VAL*
Landslide 2	0.7759	0.7415
Landslide 5	0.8596	0.6981
Landslide 7	0.7486	0.7033
Landslide 11	0.8590	0.8251

Table 32. AUC results for study 1.5

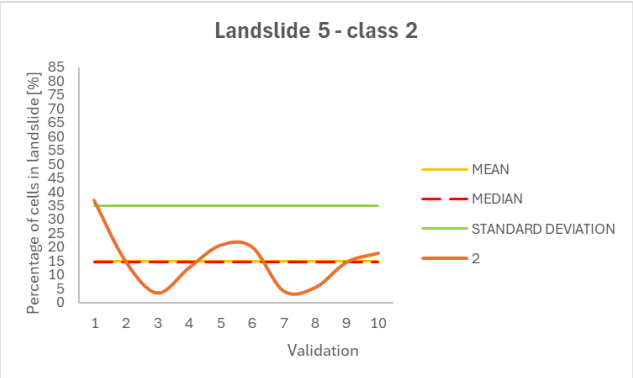

Figure 58. Mean, median and standard deviation values for landslide 5, class 2 in validation

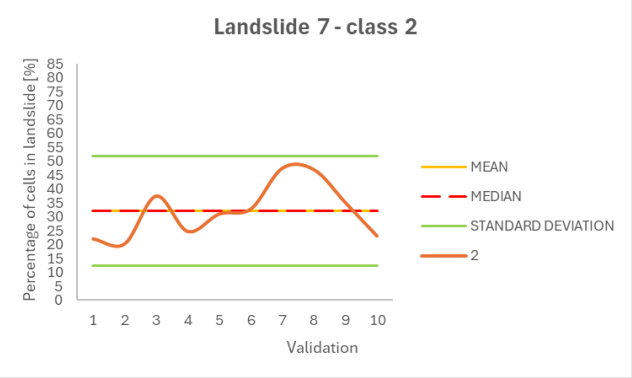

Figure 57. Mean, median and standard deviation values for landslide 7, class 2 in validation

4.7.1 Phase 2 considerations

Analysis of the results highlights significant differences between the model's calibration and validation phases for the various types of landslide considered. In particular, the model's performance is very satisfactory in the case of landslide 11, whilst it appears decidedly less effective for landslide 7.

The analysis that yielded the best results was the one conducted across the entire Metropolitan City of Genoa, highlighting how the use of a larger analysis area allows for more reliable results. This confirms that a larger geographical scope, and therefore greater data availability, helps to improve the statistical robustness of the analysis and the overall quality of the results obtained.

To improve the model's performance in the case of more complex landslides, it might be useful to further refine the analysis by excluding accumulation areas and focusing primarily on detachment zones, for example by using morphometric indicators such as slope concavity in the areas affected by landslides.

It should also be noted that the limited amount of data available for certain types of landslides can adversely affect the robustness of the results, leading to estimates that are not sufficiently representative. For this reason, it was decided to exclude type 0 and 4 landslides from the analysis, as there were too few of them. In general, a greater availability of data allows for more reliable and statistically significant results.

Finally, a further improvement in the analysis could be achieved by considering the removal of outliers present at the tails of the distributions for each class, in order to reduce statistical noise and make the model more stable and representative of prevailing conditions.

5. CONCLUSIONS

Landslide susceptibility is a topic of great scientific and practical importance, still the subject of methodological development and in-depth study in geomorphological research. In particular, this field takes on even greater importance in complex and heavily urbanised areas such as Genoa, characterised by steep slopes, a deeply incised river network, and lithological and morphological conditions that make the area particularly prone to instability phenomena. In this context, the aim of this research was to analyse and assess landslide susceptibility in the study area by integrating various morphological and environmental factors and applying data processing and modelling procedures. The approach adopted made it possible to identify the variables most influential in the area's susceptibility to landslides and to assess the effectiveness of the various model configurations in representing the spatial distribution of landslides.

The results obtained highlight how certain parameters, particularly those related to slope morphology, are decisive in determining susceptibility. In particular, the introduction of the morphological aggressiveness index has helped to improve the model's ability to describe the terrain's predisposition to instability phenomena. The configuration using 6 classes of aggressiveness and 5 classes of susceptibility showed the most satisfactory performance, providing a more consistent and realistic representation of the areas potentially prone to landslides within the analysed area. Furthermore, it highlighted that using a larger analysis area allows for more reliable results.

Overall, the best result obtained from the iterative application of the method (10 runs) pertains to the study conducted across the entire territory of the Metropolitan City of Genoa (Study 2.2). Specifically, for areas subject to widespread surface landslides, average values for the highest susceptibility class (class 5) were recorded at 51,569 during the calibration phase and 49,380 during the validation phase.

The analysis also highlighted some critical issues related to both data management and the large number of different types of landslides considered. In particular, the presence of classes characterised by a very limited number of events can affect the stability of the results and reduce the reliability of statistical estimates. For this reason, greater data availability and a more accurate selection of variables are fundamental elements for improving the robustness of susceptibility analyses and the predictive capacity of the models applied.

Overall, the study has produced a landslide susceptibility map useful for understanding the distribution of instability phenomena and for supporting land-use planning, risk management and prevention activities in a fragile territory such as that of Genoa. Further research developments could focus on improving analysis procedures for complex landslides, a particularly relevant issue in the Ligurian region. In this regard, it might be useful to deepen the analysis by distinguishing more clearly between areas of detachment and areas of accumulation—for example, by excluding the

latter or analysing them separately—and by integrating additional morphometric indicators, such as slope concavity, in order to further refine the representation of instability processes and improve the reliability of susceptibility assessments.

REFERENCES

Aleotti, P., C Chowdhury, R. (1999). Landslide hazard assessment: Summary review and new perspectives. *Bulletin of Engineering Geology and the Environment, 58*(1), 21–44. https://doi.org/10.1007/s100640050066

Akgun, A., C Türk, N. (2011). Landslide susceptibility mapping by statistical and deterministic methods: A comparison study. *Environmental Earth Sciences, c4*(3), 705–718. https://doi.org/10.1007/s12665-010-0860-0

Ayalew, L., C. Yamagishi, H. (2005). The application of GIS-based logistic regression for landslide susceptibility mapping in the Kakuda–Yahiko Mountains, Central Japan. *Geomorphology, vol. 5*(1–2), 15–31. https://doi.org/10.1016/j.geomorph.2004.06.010

Baum, R. L., Savage, W. Z., C Godt, J. W. (2002). TRIGRS—A Fortran program for transient rainfall infiltration and grid-based regional slope-stability analysis. *U.S. Geological Survey Open-File Report 02–424*.

Bonham-Carter, G. F., Agterberg, F. P., C Wright, D. F. (1989). Weights of evidence modelling: A new approach to mapping mineral potential. *Statistical Applications in the Earth Sciences*, 171–183.

Brenning, A. (2005). Spatial prediction models for landslide hazards: Review, comparison and evaluation. *Natural Hazards and Earth System Sciences, 5*, 853–862. https://doi.org/10.5194/nhess-5-853-2005

Buecchi, E., Raspini, F., Rossi, G., et al. (2019). Landslide susceptibility mapping using persistent scatterer interferometry and GIS-based models. *Geomatics, Natural Hazards and Risk, 10*(1), 170–193. https://doi.org/10.1080/19475705.2018.1505665

Canuti, P., Focardi, P., C Garzonio, C. A. (1979). Landslide hazard map and slope stability map. *Proceedings of the Italian Geological Society, 1S*, 101–114.

Cardinali, M., Reichenbach, P., Guzzetti, F., et al. (2002). A geomorphological approach to landslide hazard assessment and zonation. *Geomorphology, 31*(1–4), 181–216. https://doi.org/10.1016/S0169-555X(99)00096-1

Cascini, L. (2008). Applicability of landslide susceptibility and hazard zoning at different scales. *Engineering Geology, 102*(3–4), 164–177. https://doi.org/10.1016/j.enggeo.2008.03.016

Carrara, A., Cardinali, M., Guzzetti, F., C Reichenbach, P. (1995). GIS technology in mapping landslide hazard. In A. Carrara, C F. Guzzetti (Eds.), *Geographical information systems in assessing natural hazards* (pp. 135–175). Springer. https://doi.org/10.1007/978-94-015-8404-3_8

Chen, W., Li, X., Wang, Y., Chen, G., C Liu, S. (2018). Landslide susceptibility mapping using GIS-based machine learning methods. *Remote Sensing, 10*(10), 1520. https://doi.org/10.3390/rs10101520

Chen, W., Pourghasemi, H. R., C Naghibi, S. A. (2017). A comparative study of landslide susceptibility maps produced using support vector machines with different kernel functions and entropy data mining models. *Geomorphology, 280*, 224–241. https://doi.org/10.1016/j.geomorph.2016.12.022

Chung, C. J. F., C. Fabbri, A. G. (1999). Probabilistic prediction models for landslide hazard mapping. *Photogrammetric Engineering & Remote Sensing, 5*(12), 1389–1399. https://www.researchgate.net/publication/209802926_Probabilistic_prediction_models_for_landslide_hazard_map-ping

Civil Protection Department. (n.d.). *The Genoa flood* [Web page]. Presidency of the Council of Ministers – National Service, Department of Civil Protection. Retrieved 15 March 2026, from https://servizionazionale.protezionecivile.gov.it/en/pagina-base/lalluvione-di-genova-0/

Climate of Genoa. (3 February 2026). In *Wikipedia*. https://it.wikipedia.org/wiki/Clima_di_Genova

Municipality of Genoa. (n.d.). Climate and microclimate. Climatic characteristics of the municipality of Genoa [PDF]. https://www2.comune.genova.it/sites/default/files/DEF/1_DF/1_01_doc.pdf

Corominas, J., van Westen, C., Frattini, P., Cascini, L., Malet, J. P., Fotopoulou, S., … Hervás, J. (2014). Recommendations for the quantitative analysis of landslide risk. *Bulletin of Engineering Geology and the Environment, 73*(2), 209–263. https://doi.org/10.1007/s10064-013-0538-8

Cruden, D. M. (1991). A simple definition of a landslide. *IAEG Bulletin, 43*, 27–29.

Cruden, D. M., C. Varnes, D. J. (1996). Landslide types and processes. In A. K. Turner, C. R. L. Schuster (Eds.), *Landslides: Investigation and mitigation* (pp. 36–75). National Academy Press.

Crozier, M. J. (1986). Landslides: Causes, consequences and environment. Croom Helm.

CNR – Istituto di Ricerca per la Protezione Idrogeologica (IRPI). *Suscettibilità da frana*. https://www.irpi.cnr.it/focus/suscettibilita-da-frana/

CNR – Research Institute for Hydrogeological Protection (IRPI). *Hydrological data – Hydrogeological Disasters Information System (SICI)*. https://sici.irpi.cnr.it/idrologici.htm

Legislative Decree No. 1 of 2 January 2018. (2018). *Civil Protection Code*. Official Gazette of the Italian Republic.

Department of Civil Protection – Presidency of the Council of Ministers. *What is risk?* https://www.protezionecivile.gov.it/it/approfondimento/che-cos---il-rischio-/

Department of Civil Protection – Presidency of the Council of Ministers. *Landslides*. https://www.protezionecivile.gov.it/it/approfondimento/frane/

De Fazio, M. (19 January 2023). Landslide on Via Capolungo in Genoa, shocking report nine years on: 'Slope at risk of collapse'. *Il Secolo XIX*. https://www.ilsecoloxix.it/genova/2023/01/19/news/frana_di_via_capolungo_a_genova_perizia_choc_dopo_nove_annipendio_a_rischio_collasso-12591917/

Duncan, J. M., Wright, S. G., Brandon, C., T. L. (2014). *Soil strength and slope stability* (2nd ed.). John Wiley & Sons.

Faccini, F., Luino, F., Paliaga, G., Sacchini, A., and Turconi, L. (2015). Yet another catastrophic flood of the Bisagno stream in Genoa (Liguria, Italy): the event of 9–10 October 2014. *Rendiconti Online Della Società Geologica Italiana, 35*, 128–131. doi:10.3301/ROL.2015.81

Faccini, F., Luino, F., Sacchini, A., Turconi, L. (2015b). Flash flood events and urban development in Genoa (Italy): lost in translation. In G. Lollino (Ed.), *Engineering geology for society and territory, volume 5* (pp. 797–801). Springer International Publishing.

Faccini, F., Paliaga, G., Piana, P., Sacchini, A., C Watkins, C. (2016). The Bisagno stream catchment (Genoa, Italy) and its major floods (1822, 1970 and 2014): geomorphic and land use variations in the last three centuries. *Geomorphology, 273*, 14–27. https://doi.org/10.1016/j.geomorph.2016.07.037

AMGA Foundation. *FACCINI Project. Project report*. https://www.fondazioneamga.org/wp-content/uploads/2023/06/Progetto-FACCINI.pdf

RETURN Foundation. *Multi-Risk science for resilient communities under a changing climate*. https://www.fondazionereturn.it/

GeoEnv. *Landslides*. https://www.geoenv.it/lezioni/frane.htm

GeoPortal of the Municipality of Genoa. https://mappe.comune.genova.it/MapStore2/#/viewer/699

Guzzetti, F., Carrara, A., Cardinali, M., C Reichenbach, P. (1999). Landslide hazard evaluation: a review of current techniques and their application in a multi-scale study, Central Italy. *Geomorphology, 31*(1–4), 181–216. https://doi.org/10.1016/S0169-555X(99)00078-X

Guzzetti, F., Reichenbach, P., Cardinali, M., Galli, M., C Ardizzone, F. (2005). Probabilistic landslide hazard assessment at the basin scale. *Geomorphology, 72*(1–4), 272–299. https://doi.org/10.1016/j.geomorph.2005.06.002

Guzzetti, F., Reichenbach, P., Cardinali, M., Galli, M., C Ardizzone, F. (2007). Probabilistic landslide hazard assessment at the basin scale. *Geomorphology, 72*(1–4), 272–299. https://doi.org/10.1016/j.geomorph.2005.06.002

Guadalupo, D. *Assessment of landslide susceptibility in the Trunca catchment (RC), chapter: Concept of susceptibility*. https://bookdown.org/guadalupo_do/tesi/concetto-di-suscettibi-lit%C3%A0.html

Hungr, O., Leroueil, S., C. Picarelli, L. (2014). The Varnes classification of landslide types: an update. *Landslides, 11*, 167–194.

Hoek, E., C Bray, J. (1981). *Rock slope engineering* (3rd ed.). Institution of Mining and Metallurgy.

Iadanza, C., C. Trigila, A. (2016). Hazard and risk. *ISPRA – National Institute for Environmental Protection and Research* , presentation of 2 March 2016. https://www.isprambiente.gov.it/files/eventi/eventi-2016/frane-alluvioni/Iadanza_Trigila_Pericolosita_Rischio_ISPRA_2_marzo_2016.pdf

Italy. (2006). *Legislative Decree No. 152 of 3 April 2006: Environmental regulations.* Official Gazette of the Italian Republic.

Italy (1989). *Law No. 183 of 18 May 1989. Regulations for the organisational and functional reorganisation of soil protection.* Official Gazette of the Italian Republic, No. 120 of 25 May 1989.

ISTAT (2024). https://www.isprambiente.gov.it/files2025/pubblicazioni/rapporti/rapporto_ispra_dissesto_idrogeologico_ed2024_web.pdf

ISPRA. (2015). *Guidelines for the assessment of landslide hazard and risk*. Higher Institute for Environmental Protection and Research.

ISPRA. (2021). *Inventory of Landslide Phenomena in Italy (IFFI): methodology and current status*. ISPRA.

ISPRA and the Italian Geotechnical Association. (2016). *Guidelines for landslide risk mitigation*. AGI/ISPRA.

LabGeomatica. *SALSA.1 – Spatial Analysis for Landslide Susceptibility Assessment*, software repository, GitHub. https://github.com/LabGeomatica/SALSA.1

The Province of Varese. (5 November 2011). Bad weather/ In 50 years in Genoa: 5 landslides and 6 floods: 78 victims. *The Province of Varese*. https://www.laprovinciadivarese.it/maltempo-in-50-anni-a-genova-5-frane-e-6-esondazioni78-vittime-191607/

MeteoPresila. *Landslides: classification of landslide movements*. https://www.meteopresila.it/frane-classificazione-dei-movimenti-franosi/

Metternicht, G., Hurni, L., C Gogu, R. (2005). Remote sensing of landslides: An analysis of the potential contribution to landslide hazard assessment in mountainous environments. *Remote Sensing of Environment, S8*(2–3), 284–303. https://doi.org/10.1016/j.rse.2005.08.004

Montgomery, D. R., C. Dietrich, W. E. (1994). A physically based model for the topographic control on shallow landsliding. *Water Resources Research, 30*(4), 1153–1171. https://doi.org/10.1029/93WR02979

Neuhäuser, B., Damm, B., C Terhorst, B. (2012). GIS-based assessment of landslide susceptibility based on the weight-of-evidence model. *Landslides, S*, 511–528. https://doi.org/10.1007/s10346-011-0305-5

Paliaga, G., Luino, F., Turconi, L., C Faccini, F. (2018). Inventory of geo-hydrological phenomena in the municipality of Genoa (NW Italy). *Journal of Maps, 14*(2), 348–356. https://doi.org/10.1080/17445647.2018.1535454

Paliaga, G., Terrone, M., Bazzurro, N., Marchese, A., C Faccini, F. (2019). Rainfall-induced shallow landslide susceptibility for risk management of underground services in a Mediterranean metropolitan city. *Natural Hazards and Earth System Sciences*. https://doi.org/10.5194/nhess-19-2121-2019

Paliaga, G., Terrone, M., Bazzurro, N., Marchese, A., C Faccini, F. (2025). Rainfall-induced shallow landslide susceptibility for risk management of underground services in a Mediterranean metropolitan city. *Land, 14*(11), 2118. https://doi.org/10.3390/land14112118

Legambiente ClimaCittà Report. (2021). Genoa. https://www.genovatoday.it/cronaca/rapporto-legambiente.html

Reid, M. E., Christian, S. B., Brien, D. L., Henderson, S. T., C Grimm, C. (2015). Scoops3D—Software to analyse 3D slope stability throughout a digital landscape. *U.S. Geological Survey Techniques and Methods, Book 14, Chapter A1*.

Reichenbach, P., Rossi, M., Malamud, B. D., Mihir, M., C Guzzetti, F. (2018). A review of statistically-based landslide susceptibility models. *Earth-Science Reviews, 180*, 60–91. https://doi.org/10.1016/j.earscirev.2018.03.001

Liguria Region. (n.d.). [Specific page title]. https://share.google/ZqbVtQhRnrs7Fr0E5

Rossi, M., Reichenbach, P., C Guzzetti, F. (2010). Landslide susceptibility mapping using GIS-based statistical models. *Natural Hazards, 52*, 1–23. https://doi.org/10.1007/s11069-009-9379-2

SNPA. (2021). *Guidelines for landslide monitoring (SNPA Guidelines No. 32/2021).* National System for Environmental Protection.

Soeters, R., C van Westen, C. J. (1996). Slope instability recognition, analysis, and zonation. In A. K. Turner, C. R. L. Schuster (Eds.), *Landslides: Investigation and mitigation* (pp. 129–177). Transportation Research Board. https://onlinepubs.trb.org/Onlinepubs/sr/sr247/sr247-008.pdf

Spiegelhalter, D. J. (1986). Probabilistic prediction in patient management and clinical trials. *Statistics in Medicine, 5*(5), 421–433. https://doi.org/10.1002/sim.4780050506

Tengfei Wang, Dahal, A., Fang, Z., van Westen, C., Yin, K., Lombardo, L. (2024). From spatio-temporal landslide susceptibility to landslide risk forecast. *Geoscience Frontiers, 15*(2), 101765. https://doi.org/10.1016/j.gsf.2023.101765

Terzaghi, K., Peck, R. B., C Mesri, G. (1996). *Soil mechanics in engineering practice* (3rd ed.). John Wiley & Sons.

Umar, Z., Pradhan, B., Ahmad, A., Jebur, M. N., C Tehrany, M. S. (2014). Earthquake-induced landslide susceptibility mapping using an integrated ensemble frequency ratio and logistic regression models in West Sumatra Province, Indonesia. *Catena, 118*, 124–135. https://doi.org/10.1016/j.catena.2014.02.005

van Westen, C. J., Castellanos, E., C Kuriakose, S. L. (2006). Spatial data for landslide susceptibility, hazard, and vulnerability assessment: an overview. *Engineering Geology, 102*, 112–131.

van Westen, C. J., Castellanos, E., C. Kuriakose, S. L. (2008). Spatial data for landslide susceptibility, hazard, and vulnerability assessment: an overview. *Engineering Geology, 102*(3–4), 112–131. https://doi.org/10.1016/j.enggeo.2008.03.010

van Westen, C. J., Rengers, N., C. Soeters, R. (2003). Use of geomorphological information in indirect landslide susceptibility assessment. *Natural Hazards, 30*, 399–419. https://doi.org/10.1023/B:NHAZ.0000007097.42735.9e

Varnes, D. J. (1978). Slope movement types and processes. In R. L. Schuster and R. J. Krizek (Eds.), *Landslides: Analysis and control* (pp. 11–33). National Academy of Sciences.

Varnes, D. J. (1984). *Landslide hazard zonation: a review of principles and practice*. Commission on Landslides of the IAEG, UNESCO, Natural Hazards, 3, 61 pp.

Yilmaz, I. (2009). Landslide susceptibility mapping using frequency ratio, logistic regression, artificial neural networks and their comparison: A case study from Kat landslides (Tokat–Turkey). *Computers & Geosciences, 35*(6), 1125–1138. https://doi.org/10.1016/j.cageo.2008.08.007

Appendix

1. Characteristics of landslide phenomena

The following characteristics can be distinguished in a landslide event (Fig. 1) [3]:

1. Crown (1): material that has remained largely in place (not subject to displacement) at the top of the 'main scarp'
2. Main scarp (2): a generally steep surface delimiting the largely undisturbed area surrounding the top of the landslide, generated by the movement of the displaced material (13). It represents the visible part of the failure surface (10)
3. Top (3): the highest point of contact between the displaced material (13) and the main scarp
4. Head (4): the highest parts of the landslide along the contact between the displaced material and the main scarp
5. Main scarp (5): steep upper section present on the displaced material of the landslide, produced by different movements within the displaced material
6. Main body (6): the part of the displaced material covering the failure surface (10) between the main scarp and the toe of the failure surface (11)
7. Foot (7): the portion of the landslide that has moved beyond the toe of the failure surface and covers the original surface of the slope (20)
8. Lower tip (8): the point of the toe (9) furthest from the summit (3) of the landslide
9. Toe (9): the lower, generally curved edge of the displaced landslide material, situated furthest from the main slope
10. Surface of rupture (10): the surface that forms (or formed) the lower boundary of the displaced material beneath the original slope surface. The idealised surface of rupture may be defined as the slip surface
11. Toe of the surface of rupture (11): intersection (usually buried) between the lower part of the landslide's failure surface and the original slope surface
12. Surface of separation (12): part of the original slope surface covered by the toe (7) of the landslide
13. Displaced material (13): material moved from its original position on the slope due to the landslide movement. It forms both the detached mass (17) and the deposit (18)
14. Zone of depletion (14): the part of the landslide within which the displaced material lies below the original slope surface
15. Zone of accumulation (15): the part of the landslide within which the displaced material lies above the original slope surface
16. Depletion (16): the volume bounded by the main scarp, the detached mass (17) and the original slope surface

17. Depletion mass (17): the volume of displaced material covering the failure surface and lying below the original slope surface

18. Accumulation (18): the volume of displaced material lying above the original slope surface

19. Flank (19): undisturbed material adjacent to the edges of the failure surface. Flanks can be identified by the azimuth measured with a compass or by the terms ‘right’ and ‘left’, as seen by someone looking at the landslide from the crown (1)

20. Original ground surface (20): the surface of the slope that existed before the landslide occurred

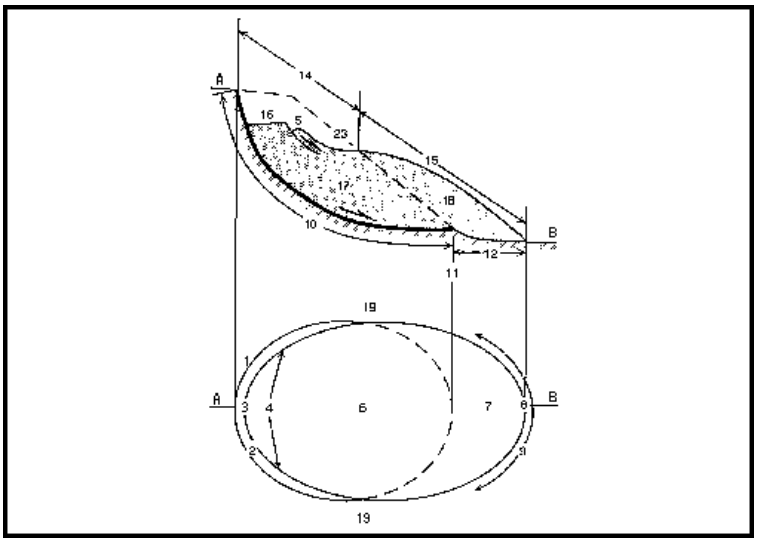

Figure 44: Characteristics of landslides (source: https://www.geoenv.it/lezioni/frane.htm)